Clinicopathologic Relevance of Vascular Changes Associated with Transplant Glomerulopathy Secondary to Chronic Antibody-mediated Rejection in the Renal Allograft

Deján Dobi, MD

PhD Thesis

Szeged, 2018

Clinicopathologic Relevance of Vascular Changes Associated with Transplant Glomerulopathy Secondary to Chronic Antibody-mediated Rejection in the Renal Allograft

PhD thesis

Deján Dobi, MD

Szeged, 2018

Department of Pathology, Faculty of Medicine,
University of Szeged

Thesis supervisor: Béla Iványi, MD, DSc

Doctoral School of Clinical Medicine

This PhD thesis is based on the following publications:

I. Dobi D, Bodó Z, Kemény É, et al. Morphologic features and clinical impact of arteritis concurrent with transplant glomerulopathy. *Pathol Oncol Res.* 2015; 22: 15–25. **(Original Research Article) IF: 1,736**

II. Dobi D, Tatapudi V, Rajalingam R, et al. Quantitative changes of kidney microvasculature in transplant glomerulopathy *Virchows Arch.* 2015; 467:S34. **(Abstract of an Oral Presentation)**

III. Dobi D, Bodó Z, Kemény É, et al. Peritubular capillary basement membrane multilayering in early and advanced transplant glomerulopathy: quantitative parameters and diagnostic aspects. *Virchows Arch.* 2016; 469: 563-573. **(Original Research Article) IF: 2,848**

Table of Contents

List of Abbreviations

ABMR, antibody-mediated rejection

Banff cv, arterial luminal narrowing due to intimal fibrosis

Banff g, glomerulitis

Banff ptc, peritubular capillaritis

BM, basement membrane

CI, confidence interval

cv_{IF}, intimal fibrosis without leukocytes

$cv_{IFE,}$ intimal fibroelastosis

cv_{mo}, fibrosing intimal arteritis

C4d, complement 4d

DSA, donor-specific alloantibody

EFg, glomerular endothelial fenestra

EM, electron microscopy

FS, filtration slit

GBM, glomerular basement membrane

GBM_{den}, length of the portion of peripheral capillary loop that is affected by endothelial detachment

$GBM_{dep,}$ length of the portion of peripheral capillary loop that is affected by epithelial detachment

$GBM_{l,}$ length of the peripheral segment of the glomerular capillary loop

HCV, hepatitis C virus infection

HLA, Human Leukocyte Antigen

IC, immune complex

Ig, immunoglobulin

IHC, immunohistochemistry

IQR, interquartile range

MFI, mean fluorescent intensity

mTOR, mechanistic target of rapamycin

MVI, microvascular inflammation

NK-cell, natural killer cell

PAS, periodic acid-Schiff

PRA, panel reactive antibody

PTC, peritubular capillary

PTCBMML, peritubular capillary basement membrane multilayering

ROC-curve, receiving operator characteristics curve

RT, renal transplantation

TIA-1, T-cell intracellular antigen

TxG/Banff cg, transplant glomerulopathy

UCSF, University of California, San Francisco

$\delta_{GBM,}$ mean harmonic glomerular basement membrane thickness

List of Figures

Disclosure:

Figure 1 has been published before in Ivanyi B, Kemeny E, Szederkenyi E et al. The value of electron microscopy in the diagnosis of chronic renal allograft rejection. *Modern Pathol.* 2001; 14: 1200-1208.

Figure 2 and 3b have been published before in Remport A, Ivanyi B, Mathe Z et al. Better understanding of transplant glomerulopathy secondary to chronic antibody-mediated rejection. *Nephrol Dial Transplant.* 2014; 30: 1825–33.

Introduction

Major Barriers to Improving Long-term Renal Transplant Survival

Renal transplantation (RT) is the recommended treatment option for patients with end stage renal disease who have no contraindication to the procedure or to post-transplant immunosuppression. It is superior to any form of prolonged dialysis in regards to quality of life, and overall survival, even after adjustment for waiting-list selection bias [1, 2]. In addition, long-term cost effectiveness of RT is also better than that of intermittent hemodialysis [3].

Although RT is the therapy of choice in an adequately selected patient pool, there is a gap between the average life expectancy of the transplanted patient population and the survival of the transplanted organ [4]. The two major causes of premature graft loss are *de novo*/recurrent non-alloimmune diseases [5, 6], and the alloimmune response against the renal transplant [7,].

Major improvements in the last four decades in the field of immunosuppression [8] resulted in a significant change in the kinetics and typical patterns of the alloimmune injury. Previously, the acute forms of rejection [especially acute T-cell mediated rejection (TCMR)] were responsible for the majority of graft failures [9]. This had changed upon the introduction of T-cell signaling pathway-antagonists [10], inhibitors of mechanistic target of rapamycin (mTOR) [11], and T-cell metabolic toxins [12] that increased the 1 year graft survival to 90 % by the early 2000's [4, 9].

In contrast, the long-term renal allograft survival is still limited, approximately 50 % of the transplanted patients lose their kidney within 10-12 years after transplantation [4]. While chronic allograft dysfunction is multifactorial, the main reason of late allograft loss is chronic antibody-mediated rejection (ABMR) [13] that triggers progressive injury of the graft vasculature via donor-specific alloantibodies (DSAs) [14]. DSAs lead to injury, activation and subsequent repair of the endothelial lining [15]. The net result of these events is luminal narrowing of the graft arteries and the remodeling of the microcirculation [16]. The major morphological change is glomerular double contours (transplant glomerulopathy - TxG) and

peritubular capillary basement membrane multilayering (PTCBMML) [17-20]. Clinically, slowly declining graft function, and proteinuria develop that eventually lead to graft failure [21].

Transplant Glomerulopathy - Prevalence and Prognosis

Transplant glomerulopathy is a long-term complication of renal transplantation. In a dysfunctional biopsy series by Sis *et al* the light-microscopic diagnosis of TxG was established at a median of 5.5 years post-transplant [16]. Most studies reported a prevalence of the condition (as assessed by light microsopy) between 1.6 to seven percent in unselected biopsy series [22-25]. The true prevalence is probably higher, since many patients with late-onset allograft dysfunction do not undergo biopsy procedure. There is a strong connection between de novo DSAs and TxG [26], furthermore, crossmatch positivity also increases the probability of the condition [27].

Transplant glomerulopathy has a major impact on graft survival: Sellares *et al* studied 315 renal allograft recipients prospectively. Among the 56 graft failures that occurred during the study period, 46 percent of grafts showed TxG [13]. Kieran *et al* described a cohort of 78 patients with late allograft dysfunction (more than 10 years after transplantation) and found the three year post-biopsy graft survival to be 32 percent in patients with TxG compared to 82 percent in patients without TxG [28]. Einecke and Sis studied more than 150 unselected renal transplant patients prospectively who underwent for-cause biopsy [29]. They found that 26 percent of grafts with dysfunctional biopsies over one year after transplantation progressed to failure within three years after the biopsy. Sixty-three percent of the patients who lost their allograft had microcirculation changes (including TxG) and were positive for DSA. Glomerulonephritis, drug toxicity, acute TCMR were a lot less common cause of graft failure. [29]

While grafts with TxG have worse survival compared to those without, several co-factors can modify outcomes for patients with the condition. Determinants of allograft failure once TxG is established are: increased serum creatinine [30, 31] increased urine protein to creatinine ratio [31, 32] presence and class of DSAs, [33-35] higher grades of interstitial fibrosis/tubular

atrophy [30, 31, 36], complement 4d (C4d) deposition around the peritubular capillaries [28, 34-36] and increased level of endothelial transcripts [32].

Pathomechanism of Transplant Glomerulopathy

Overview

Transplant glomerulopathy, although shows a strong pathogenic connection with DSAs, is not specific to ABMR [18, 19]. The lesion is a pathologic pattern and not a disease entitiy and it is considered to be the final common pathway of endothelial injury and remodeling due to a wide variety of damaging effects. The most frequent non-alloimmune causes that lead to TxG are thrombotic microangiopathy, and membranoproliferative glomerulonephritis [due to Hepatitis C virus (HCV) infection or other causes] [37]. Since our work analyzes the prognostic factors associated with TxG due to ABMR, only the pathomechanism of glomerular double-contouring secondary to DSAs will be discussed in the following sections.

Effector Functions of the Alloantibodies

Donor-specific antibodies that are most often associated with the development of TxG are directed against class II Human Leukocyte Antigens (HLA) [38-40]. DSAs damage the endothelial lining of the transplanted organ's vasculature via three effector functions: (I) activation of classical complement cascade, (II) engaging Fc-receptors on myeloid and lymphoid cells, and (III) cross-linking of HLA antigens, that triggers downstream activation of the target cell [41].

Activation of the classical complement pathway starts with the binding of C1q to the Fc portion of the DSA that is already bound to an allogenic HLA. This initiates the complement cascade which results in the formation of the membrane attack complex leading to the (sub)lytic injury of the cell [42], and the generation of complement fragments that stimulate inflammatory responses (C5a, C4a, and C3a). Endothelial cells express complement regulatory proteins (CD55/DAF, Crry, CD59) that inhibit the effects of the complement activity, while further

cleavage products are generated (e.g. C4d and C3d). Complement 4d binds covalently to the endothelial cell and its presence can be detected by immunohistochemistry (IHC) that serves as an immunopathologic evidence of alloantibody action against the graft endothelium [43].

Fc receptors against different immunoglobulin (Ig) heavy chain classes can be found on a wide variety of myeloid and lymphoid cells. Since DSAs prominently belong to the IgG class, the most relevant receptors in the context of alloimmune response are Fcγ receptors (CD16, CD32 and CD64) that are expressed by members of the monocyte-macrophage system, neutrophil granulocytes, and natural killer (NK) cells [41]. Upon interaction with the Fc portion, they become cross-linked and induce intracellular signaling in the immune cell that leads to its activation and maturation, and mediates effector functions [41]. An important effector function is the alloantibody-dependent cellular cytotoxicity triggered by the interaction of CD16 and the allogenic HLA-DSA immune-complex on the endothelial surface [44, 45]. This initiates secretion of perforin and granzyme that leads to endothelial injury and interferon-γ secretion via T-bet activation [46, 47].

Crosslinking of allogenic HLA by DSAs results in the activation of mTOR and mitogen-activated protein kinase signaling [48]. These pathways promote cell survival [49, 50] and prevent endothelial cells from cell death triggered by complement activation [51], respectively. Cross-linked HLA-I also couples with integrin β4 that plays an important role in cytoskeletal organization, cell adhesion, migration, and proliferation [52]. The consequence of these functional-structural alterations is Janus-faced: while pro-survival and cell-growth signals are effective in maintaining the endothelial barrier they may also contribute to the remodeling of the intimal layer of the large vessels and of the microvascular basement membrane (BM). In addition, the Ca-influx triggered by HLA cross-linking leads to the exocytosis of Weibel-Palade bodies [53, 54, 55] and consequently to increased cell surface expression of von Willebrand factor and P-selectin. The latter molecule plays an important role in leukocyte recruitment and induces the accumulation and margination of leukocytes in the microvasculature [53, 54] that manifests morphologically as glomerulitis and peritubular capillaritis (together referred to as microvascular inflammation - MVI). In the large vessels, P-selectin can also mediate transmural arteritis.

Diagnosis and Pathologic Characteristics of Transplant Glomerulopathy

Initial Morphologic Changes

In the presence of DSAs - even early after post-transplantation - ultrastructural signs of endothelial activation (endothelial swelling, loss of fenestration, and endothelial serration) can be seen by electron microscopy (EM) [56, 57]. Upon prolonged interaction between the DSAs and the endothelium, subendothelial electrolucent widening occurs and new BMs start to form. First, double contouring develops only focally and does not affect the whole circumference of the capillary loop (Figure 1). As the process progresses the lesion becomes apparent by light microscopy on sections stained with special stains that highlight the BMs (periodic acid-Schiff, methenamine silver stain).

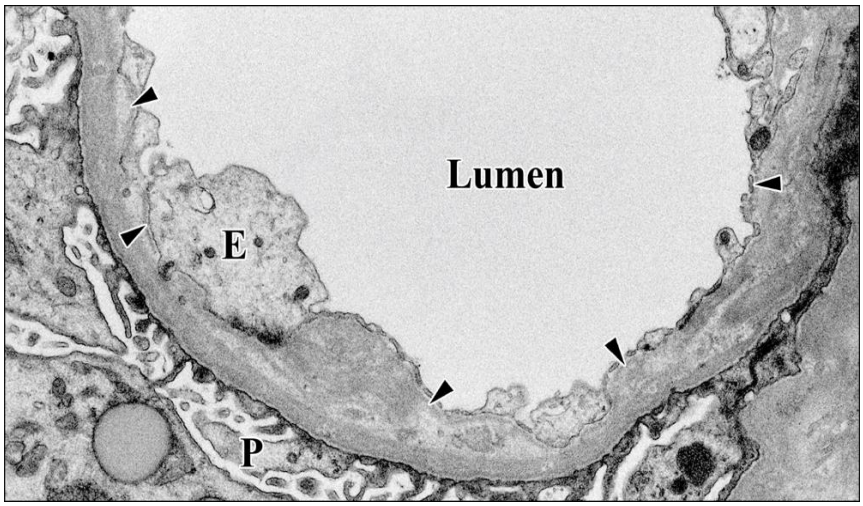

Figure 1. *Early transplant glomerulopathy by electron microscopy. Subendothelial widening, focal loss of endothelial cell fenestrations and partial duplication of the glomerular basement membrane (arrowheads). E – endothelium, P – podocyte foot processes (uranyl acetate and lead citrate stain, 9300x, courtesy of Béla Iványi, University of Szeged)*

Overt Transplant Glomerulopathy

In well-developed cases usually multiple glomeruli are involved and several loops show double contouring in the most severely affected glomerulus (Figure 2a and b) [17]. Mesangial matrix deposition, sometimes mesangial cell hypercellularity coexist with these pathologies. At the ultrastructural level, these changes can be accompanied by podocyte foot process effacement

and mesangial cell interposition. New BM formation also can be observed around the peritubular capillaries (PTC) as circumferential electrodense layers in addition to the endothelial changes similar to the glomeruli [56]. By the time the lesion becomes clinically apparent (proteinuria, declining graft function) other morphological alterations also occur: intimal fibrosis and luminal narrowing of the arteries, arteriolar hyalinosis, segmental or global glomerulosclerosis, interstitial fibrosis, and tubular atrophy can be detected [17]. Glomerulitis and peritubular capillaritis can also be present both at an early and at more advanced stages (Figure

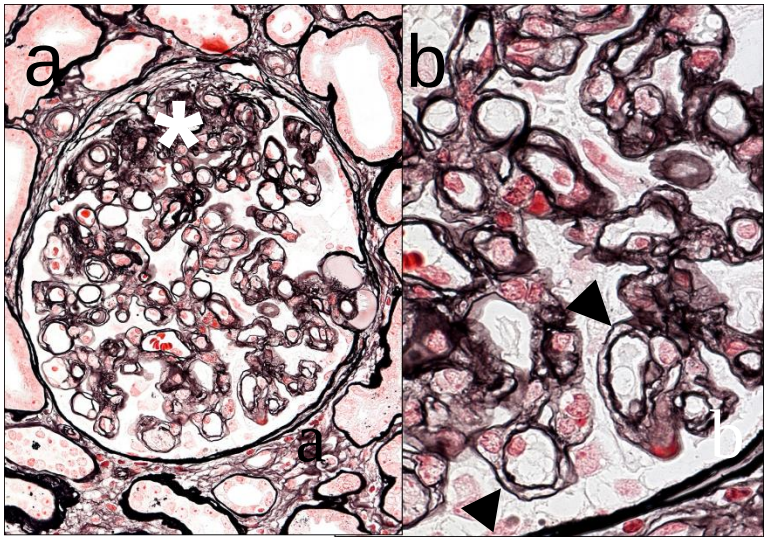

Figure 2. *Severe transplant glomerulopathy with more than 75 percent of the peripheral capillary loops showing double contours (a). Asterisk – segmental sclerosis; methenamine silver stain, 400x. Insert (b) shows glomerular double contours along the entire capillary circumference (arrowheads). Courtesy of Béla Iványi, University of Szeged.*

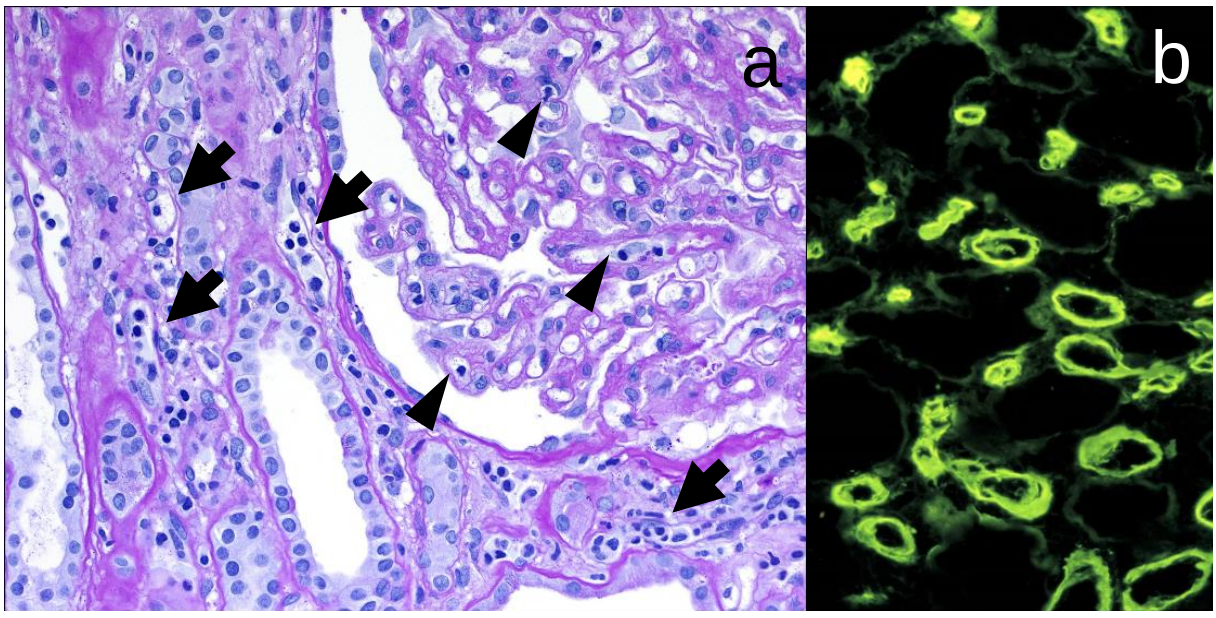

Figure 3. *Morphologic signs of donor-specific antibody-endothelium interaction. (a) Accummulation of inflammatory cells in the glomerular capillary loops (arrowheads), and peritbular capillaries (arrows). Periodic acid-Schiff stain 600x. (b) Circumferential C4d positivity around the peritubular capillaries (C4d stain, frozen section, 400x). Courtesy of Béla Iványi, University of Szeged.*

3a). As the pathomechanism of TxG due to ABMR is not immune complex (IC)-mediated, IHC studies for IgG, IgA, and C1q are negative. Infrequently, mild, mesangial/peripheral positivity can be found for IgM and C3 in the glomerulus. Linear C4d positivity around the PTCs (Figure 3b), as it have been discussed previously, indicates recent or ongoing DSA-endothelium interaction, and as such, an important part of the diagnosis of chronic active ABMR [58, 59].

Differential Diagnosis of Transplant Glomerulopathy Secondary to Antibody-mediated Rejection

Membranoproliferative glomerulonephritis or other IC-mediated pathomechanisms that lead to glomerular double contours can be excluded by IHC and EM. Chronic thrombotic microangiopathy-mediated glomerular alterations due to calcineurin-inhibitor toxicity [60] or other causes (thrombotic thrombocytopenic purpura/haemolytic uraemic syndrome, antiphospholipide syndrome) are often times indistinguishable morphologically from transplant glomerulopathy secondary to ABMR. In these cases, especially if the C4d staining is negative, and there is no MVI, correlation of the morphological findings with the patient's clinical history, laboratory results, and previous biopsy reports from the same allograft is recommended [37].

Histological Signs of Chronic Tissue Injury due to Chronic Active Antibody-mediated Rejection

Diagnostic Criteria of Chronic Active Antibody-mediated Rejection

Diagnosis of chronic active ABMR relies on the standardized histological assessment of the biopsy specimen as described by the Banff classification [61-67] (named after the Canadian city, where the first consensus meeting of a group of pathologists, nephrologists, and transplant surgeons was held on renal allograft pathology). The current version of the Banff scheme [67] requires the following criteria for the diagnosis of chronic active ABMR: (I) presence of chronic tissue damage due to alloantibodies (TxG or severe PTCBMML or arterial intimal fibrosis), (II)

evidence of current/recent alloantibody interaction with the vascular endothelium (C4d positivity, or at least moderate MVI, or increased expression of ABMR-related transcripts), and (III) serologic evidence of DSAs.

Transplant Glomerulopathy - the Cardinal Phenotype of Chronic Active Antibody-mediated Rejection

Transplant glomerulopathy (catalogued by the Banff group as cg) has long been acknowledged as a potential morphological sign of late-onset alloimmune response. In the first iteration of the Banff classification, the diagnosis of "chronic rejection" was based on the presence of cg and new onset arterial intimal fibrosis (cv lesion) [61].

Transplant glomerulopathy is one of the most specific manifestations of chronic tissue damage due to DSAs [18]. Based on the Banff classification, it is graded by the percentage of involved capillary loops in the most affected non-sclerotic glomerulus. The lesion is mild (cg1) if the double contouring affects less than 25 percent of the capillary loops, moderate if it involves 26 to 50 percent, and severe if more than 50 percent of the glomerular loops display the lesion. In 2013, the Banff classification introduced cg1a that was defined as no glomerular BM (GBM) double contours by light microscopy but GBM reduplication (incomplete or circumferential) in at least three glomerular capillaries by EM, with associated endothelial swelling and/or subendothelial electrolucent widening. Simultaneously, Banff cg1 was renamed to Banff cg1b [65]. Although the role of the ultrastructural examination in the early diagnosis of TxG was extensively studied [56, 57], little is known about the prognostic relevance of electron microscopic changes seen in TxG.

Arterial Intimal Fibrosis - a Morphological Sign of a Wide Variety of Conditions

Banff cv can be assessed by light microscopy on routinely stained sections. The lesion is mild if the narrowing does not reach 25 percent of the total luminal area, moderate if it is between 26 and 50 percent, and severe if it is above 50 percent (Figure 4). It is the least specific amongst

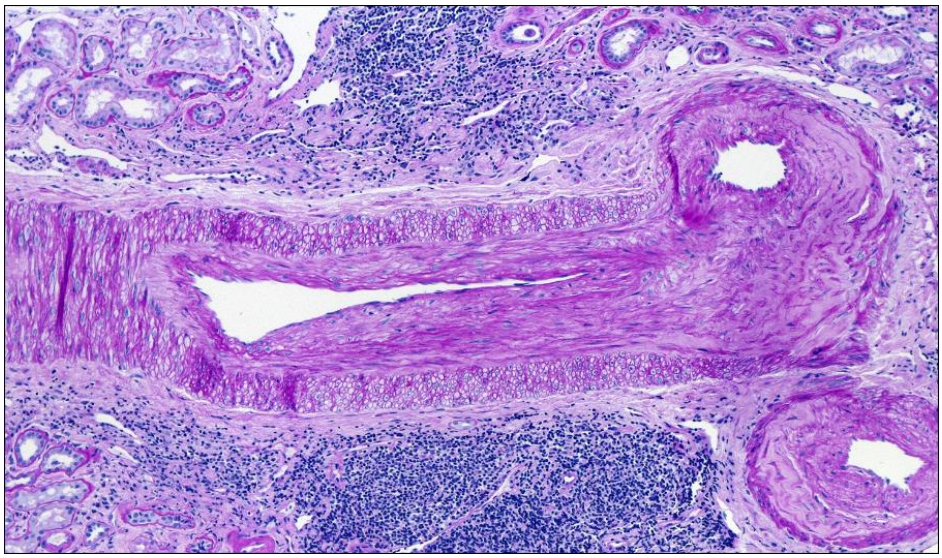

Figure 4. *Severe arterial luminal narrowing due to new onset intimal fibrosis. (periodic acid-Schiff stain, 200x). Courtesy of Béla Iványi, University of Szeged*

the signs of chronic tissue injury due to ABMR and can be a result of hypertension or aging, most frequently as an imported lesion. Presence of additional internal elastic laminas (highlighted by elastic stain) supports hypertension as the main cause of luminal narrowing. In addition, assessment of the implantation biopsy sample is crucial, and only Banff cv of new onset can be considered (after excluding other causes) as an antibody-mediated change [68]. There are morphologic alterations that favor the alloimmune nature of the lesion amongst which the most prominent is the presence of leukocytes within the fibrotic intima (fibrosing intimal arteritis) [43, 63]. The lesion can be seen in chronic ABMR and it is the defining lesion of chronic active TCMR. However, its impact on graft function and survival has not been studied yet.

Peritubular Capillary Basement Membrane Multilayering - an Ultrastructural Lesion with a Debated Threshold

Peritubular capillary basement membrane multilayering has to be assessed by EM and the lesion can only be used as a sign of antibody-mediated chronic tissue injury in the Banff classification if seven or more layers in one cortical PTC and five or more in two additional capillaries can be detected (severe PTCBMML) [65]. This ‘strict’ threshold is based on a study by Liapis *et al* [69].

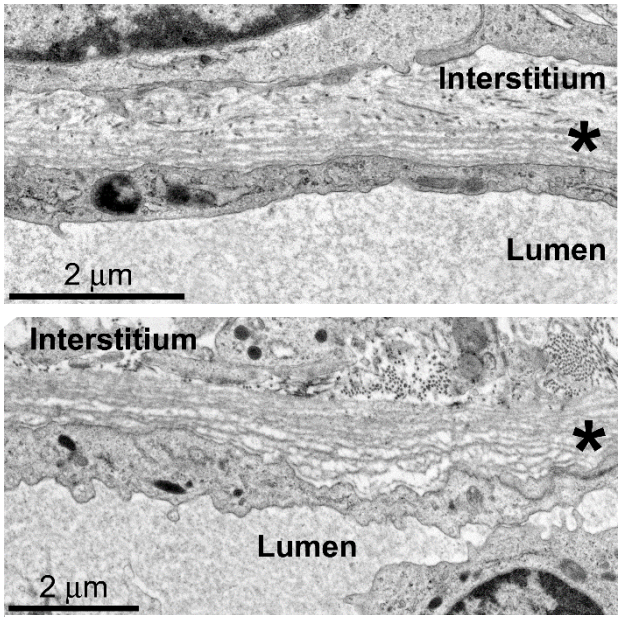

Figure 5. *Peritubular capillary basement membrane multilayering by electron microscopy. The endothelium is non-fenestrated and thickened, indicating endothelial activation; the capillary basement membrane is laminated and split (asterisk). Top: a capillary profile with five to six basement membrane layers (6000x); bottom: a profile with nine to ten layers (8000x). Lumen – lumen of the peritubular capillary, Interstitium – narrow peritubular interstitium.*

However, less pronounced PTCBMML may also be indicative of chronic ABMR in the appropriate morphologic context. When the lesion was validated in 2000 as a potential ultrastructural marker of chronic ABMR, the number of circumferential BMs around each sampled PTC, and the mean number of BM layers (PTC_{CIRC}), were recorded in biopsies displaying TxG and/or arterial intimal fibrosis, and control biopsies [70]. The study concluded that if one PTC with seven or more layers or at least three PTCs with five to six layers were noted, the lesion could be regarded as a marker of ABMR-induced tissue damage ('intermediate' threshold). Subsequent studies found [71, 72] that if thrombotic microangiopathy or obstructive uropathy (the main causes of PTCBMML other than the alloimmune response) can be excluded clinically, even one PTC with five to six layers was indicative of ABMR-induced injury ('permissive' threshold). The diagnostic importance of less pronounced PTCBMML was also emphasized by Roufousse and her co-workers who found that a PTC_{CIRC} value of 2.5 layers or greater predicted the development of TxG in patients with de novo DSA ($p = 0.001$) [73, 74]. However, it is not known whether these different thresholds for DSA-induced PTCBMML represent early or advanced stage of chronic ABMR and their utility in routine diagnosis has not yet been clarified.

Aims

To better understand the clinicopathologic relevance of macro-, and microvascular changes associated with TxG, we set the following research goals and designed three retrospective studies:

To analyze the prognostic relevance, morphological characteristics and the immunophentoype of fibrosing intimal arteritis concurrent to TxG and to investigate its relationship to other morphological alterations associated with chronic ABMR.

To describe the microvascular lesions related to TxG at the ultrastructural level by using morphometry tools and to explore the utility of the ultrastructural metrics in graft survival prognostication.

To study whether the current Banff threshold or previously proposed cut-off values for DSA-induced PTCBMML corresponds best to an early stage of chronic ABMR, and to establish a PTC_{CIRC} value typical of early and fully developed chronic ABMR.

Material and Methods

General Aspects

Renal Biopsy Sample Handling

Renal biopsy cores for light microscopic analysis were fixed in 10 percent neutral buffered formalin and embedded in paraffin. Paraffin blocks were cut, and serial, two µm thick sections were stained with haematoxylin and eosin, and with further special stains [periodic acid-Schiff (PAS), methenamine silver-periodic acid (Jones stain) or alternatively PAS-silver, Masson's trichrome, and elastic stain].

For immunofluorescence (IF) microscopy, serial sections were cut at three to four µm in a cryostat from the tissue cores submitted for freezing. Direct IF with fluorescein-labeled antibodies was performed against C3, fibrinogen, and albumin, or C3, IgG, IgA, IgM, and HLA-DR (depending on the protocol used for the particular study). Complement 4d was detected by indirect IF method with fluorescein-labeled anti-IgG secondary antibody and was part of both IF panel.

Tissue for EM was fixed in three percent phosphate-buffered glutaraldehyde. Postfixation was performed in one percent osmium tetroxide. The tissue pieces were embedded in epoxy resin, and ultrathin (90-100 nm) sections were cut and stained with lead citrate and uranyl acetate. Sections were examined by transmission EM (Tecnai G2, FEI, Hillsboro OR, USA or JEM-1400Plus, JEOL, Tokyo, Japan). Images were acquired using digital cameras (Hamamatsu Orca-HR or Ruby by JEOL) and archived as tiff files for subsequent analysis.

Sample Adequacy

Only patients with adequate samples were included in the studies. Sample adequacy criteria were adopted from the Banff classification [61] and required at least seven non-sclerosed glomeruli and one interlobular artery for light microscopy, at least four glomeruli in frozen

sections for IF microscopy, and at least one non-sclerosed glomerulus with more than 10 periglomerular PTCs for EM. If a given patient had more than one biopsy displaying TxG, the first biopsy in which cg was recorded (index biopsy) was analyzed.

Panel Reactive Antibody and Donor-specific Alloantibody Assessment

The panel reactive antibody (PRA) level was measured via a complement-dependent lymphocytotoxicity assay based on recommendations by Terasaki and McClelland [75, 76], using an in-house cell panel. DSAs were identified from the recipients' serum samples with a multiplexed assay that uses HLA antigens coupled to fluorescent beads to characterize an individual's alloantibody repertoire (single antigen bead method). Over 120 core HLA antibodies were measured using this technology (Luminex xMAP) according to the manufacturer's recommendations (One Lambda, Canoga Park, CA, USA). The results were expressed as adjusted mean fluorescence intensity (MFI), threshold to call antibodies was equal to or larger than 1000 MFI. The sample of a given patient was collected at the time of the biopsy procedure or if no such sample was available, then a sample taken at any time after the transplantation. Because of the retrospective design of our studies, testing for DSAs were not available for all cases.

Histological Assessment

All enrolled biopsy samples were assessed and graded semi-quantitatively from 0 to 3 by 2 independent observers for the presence and severity of acute and chronic lesions in the arteries, arterioles, glomeruli, PTCs, interstitium and tubuli. In the event of disagreement, a consensus score was agreed on. For the complete list of lesions and the thresholds of severity grades we refer to the 2015 Banff classification [66]. Here, we only highlight two microvascular alterations that have diagnostic relevance in chronic active ABMR in addition to Banff cg and cv. Glomerulitis (Banff g) is graded as g1 if at least a single glomerulus but not more than 25 percent of the glomeruli show leukocytic infliltrate in their capillary loops, g2 if 25 to 75 percent of the glomeruli are affected and g3 if more than 75 percent are involved. Peritubular capillaritis (Banff ptc) can be diagnosed if more than 10 percent of the PTCs show inflammatory cell

accumulation and the most severely affected capillary has at least 3-4 cells (ptc1), 5-10 cells (ptc2), or more than 10 cells (ptc3). Minor modifications to the Banff 2015 lesion and grading catalogue were applied depending on the context of the particular study, these are discussed in the sections presenting the specific features of the particular project.

Statistical Methods

Statistical analyses were performed with versions 20.0, 22.0, and 24.0 of SPSS software (IBM, Armonk, NY, USA). Continuous variables were expressed as medians with interquartile range (IQR, 25 percentile to 75 percentile) if they deviated from a normal distribution (tested by the Shapiro-Wilk test), or mean ± standard deviation. Categorical variables were presented as the count of cases. Independent samples t-test, Mann-Whitney U test, Kruskal-Wallis test, and chi-square test were used where applicable. The problem of multiple comparisons was counteracted with the Bonferroni correction. Value of $p < 0.05$ was considered significant. The morphological lesions were correlated according to Spearman's rank order.

The graft survivals were tested by medians of Kaplan-Meier curves. Graft failure was defined as the restarting of dialysis. Patient censoring was performed either at the end of the follow-up of the given study or because of death with a functioning graft or removal of the functioning graft due to reasons unrelated to the alloimmune response.

Morphologic Features and Clinical Impact of Arteritis Concurrent with Transplant Glomerulopathy

In this retrospective study, 59 patients with TxG were analyzed who underwent for-cause biopsy procedure between 2001 and 2011. The biopsy samples were selected from the renal transplant biopsy inventory of the Department of Pathology, University of Szeged based on sample adequacy and presence of glomerular double contours.

The evaluation of chronic arterial changes were modified compared to the Banff classification. We defined three categories: (I) fibrosing intimal arteritis with mononuclear cell infiltration

(cv_{mo}), (II) intimal fibrosis without inflammatory cell infiltrate (cv_{IF}), and (III) intimal fibroelastosis (cv_{IFE}, related to aging/hypertension). Intimal fibroelastosis was defined as two layers or more of internal elastic laminas seen on elastic staining. The lesions were graded based on the Banff thresholds for the cv lesion. Hierarchical cluster analysis (HCA) was used to explore the class relationships among the newly defined lesions and those part of the Banff classification [77].

Serial sections consecutive to the section in which the arteritis lesion was found were stained for CD3 (pan T-cell marker), CD68 (macrophage marker), CD8, and T-cell intracellular antigen-1 (TIA-1, marker of cytotoxic T-cells). The intimal area of the inflamed arteries was measured with an eyepiece graticule to assess inflammatory cell density in the intima.

In addition to the modifications in the light microscopic assessment, we also used a three-tired grading system for PTCBMML: with thresholds of three to four layers, five to six layers, and equal to or more than seven layers per PTC. Tubular HLA-DR expression, upregulated in acute TCMR [78, 79], was assessed on the basis of whether it was observed in at least four tubular profiles or not (scores 1 or 0, respectively).

To assess the impact of arteritis on renal function and graft survival, two groups were defined for statistical analysis: cg with arteritis and cg without arteritis. The demographic, clinical, morphological and graft survival data of the two groups were compared. To analyze the estimated glomerular filtration rate (eGFR) means over time in the two groups, we compiled the results of eGFR measurements from 36 months pre-biopsy (or, if the transplantation was performed within 36 months before the biopsy, from the time of transplantation) to 24 months post-biopsy (or, if graft failure occurred within 24 months, to the point of graft failure). Since some data were missing from our data set, the two-way mixed ANOVA model was used with time as the repeated-measures (within-subject) factor and group as the between-subject factor. Pairwise comparisons were performed on estimated marginal means by taking into account the presence of interaction. Holm-Sidak method was used for p-value correction. The interval between the repeated measures was three months. Measurements performed within one month

before or after the time of the enrolled biopsy were also included. Graft survival was tested as described under ‘General aspects’.

Quantitative Changes of the Renal Microvasculature in Transplant Glomerulopathy

This was a retrospective cohort study carried out at the Departments of Pathology, University of California, San Francisco (UCSF), and University of Szeged. Between 2007 and 2012, 164 patients admitted to UCSF who was subjected to a for-cause biopsy were found to have TxG. From these subjects, 47 patients met the sample adequacy criteria as detailed above and were not disqualified by the exclusion criteria: 1) concomitant IC glomerulonephritis or nodular/advanced diabetic glomerulosclerosis 2) history of or concurrent thrombotic thrombocytopenic purpura/haemolytic uremic syndrome 3) seropositivity for HCV.

To explore the severity of the ultrastructural lesions in TxG they were compared with normal protocol biopsies. Eleven such sample were enrolled from two transplant centers: from UCSF, five, 6-month protocol biopsies were chosen while from the Department of Pathology, University of Szeged, three 3-month, two 12-month and one 24-month protocol biopsies were selected.

In addition to the routine diagnostic workup, a detailed electron microscopic analysis of the glomeruli and the PTCs was performed in both the TxG and the protocol groups. One to two glomeruli were analyzed per sample. The median number of capillary loops/glomerulus analyzed by EM was 10 [interquartile range (IQR) = 0]. Glomeruli that were sclerosed, incomplete, or ischemic were disregarded. First, two to three, randomly selected peripheral capillary loops adjacent to each other were photographed (this area was considered to be the ‘12 o’clock position’ of the glomerular tuft). Further photographs were taken on other sets of loops at 3, 6, and 9 o’clock positions. The entire peripheral (i.e. non-mesangial) segment of each selected loop was photographed. We adopted the definition of mesangium from Wavamunno et al. [56]

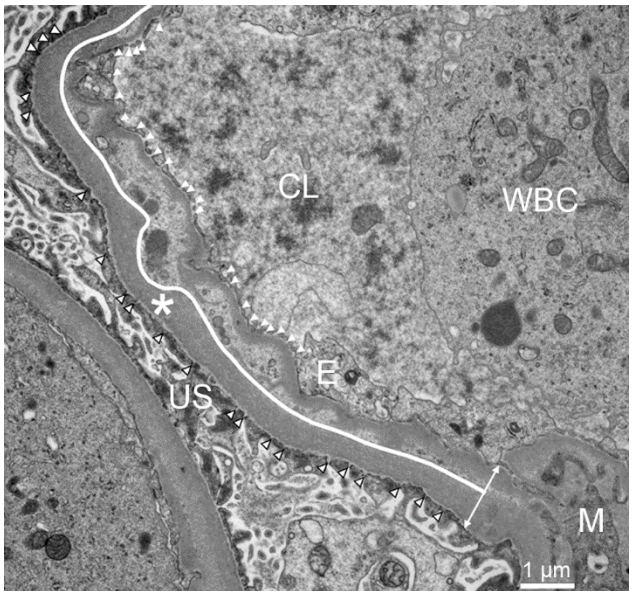

Figure 6. *Glomerular ultrastructural measurements I. Length of the peripheral segment of the capillary loop was measured (wavy line). Each endothelial fenestra (white arrowheads) and filtration slit (white arrowheads with black outline) was identified by the examiner and was counted, 9300x. CL – capillary lumen, E – endothelium, M – mesangium, US – urinary space, WBC – white blood cell. Asterisk – original lamina densa layer, Double arrow – mesangial border.*

On each photograph, the length of the peripheral segment of each capillary loop (GBM_l) was measured (Figure 6), along with the portion of the GBM affected by epithelial or endothelial detachment (GBM_{dep}, GBM_{den} respectively). We counted each filtration slit (FS) manually and defined FS frequency/loop (Figure 6.) as:

$$\frac{\Sigma FS}{GBM_l - GBM_{dep}}$$

Glomerular endothelial fenestra (EF_g) count was also recorded and EF_g frequency/loop (Figure 6) was calculated as:

$$\frac{\Sigma EF_g}{GBM_l - GBM_{den}}$$

Mean harmonic GBM thickness (δ_{GBM}) was measured with the orthogonal intercept method (Figure 7) [80]. First, a 3000 × 3000 nm line grid placed randomly on the digital image. An intercept point was defined as the intersection of the gridlines and the endothelium's membrane segment facing towards the GBM. The total BM thickness was defined as the distance from the intercept point to the epithelial cell plasma membrane in a line perpendicular to the plane of the GBM. The width of lamina rara interna was defined as the segment of the orthogonal intercept between the intercept point and the inner border of the newly formed lamina densa-like material or if such structure was not present, the original lamina densa. Mean harmonic endothelial thickness was measured by the extension of the orthogonal intercepts towards the luminal segment of the endothelium membrane (Figure 7).

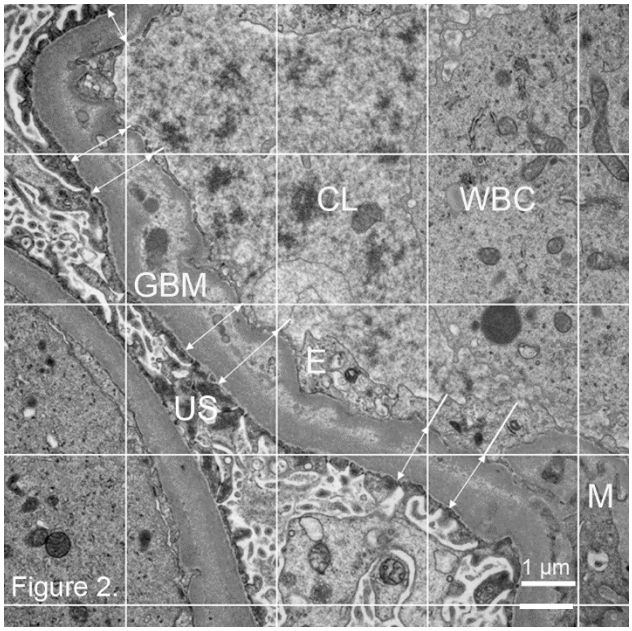

Figure 7. *Glomerular ultrastructural measurements II. A 3000 nm by 3000 nm line grid was placed on each image to measure the glomerular basement membrane (double arrows) and endothelial thickness (segments on top of double arrows). 9300x. CL – capillary lumen, E – endothelium, GBM – glomerular basement membrane, M – mesangium, US – urinary space, WBC – white blood cell.*

Peritubular capillaries in the non-scarred cortex were sampled from a random periglomerular starting point (median sample size = 10 PTC/biopsy, IQR = 1), and were analyzed for the same parameters listed above (where it was applicable) with four adjustments:

1. An intercept point was defined as every second intersection between a randomly placed 3000 × 3000 nm line grid and the PTC endothelium.
2. The orthogonal intercept was defined as the shortest distance between the intercept point and the outer border of the outermost lamina densa layer of the PTC basement membrane (PTCBM).
3. PTCBMML was expressed as mean PTC_{CIRC} in each case, based on the following formula:

$$PTC_{CIRC} = \frac{PTC_{1-2} \times 2 + PTC_{3-4} \times 4 + PTC_{5-6} \times 6 + PTC_{7-8} \times 8 + PTC_{9} \times 9}{PTC_{TOTAL}}$$

where $PTC_{1\text{-}2}$…PTC_9 are the counts of PTCs with the given number of PTCBMs, and PTC_{TOTAL} is the count of all capillaries that were examined in a given case. Only those BM layers that were observed in more than 60% of the capillary circumference (circumferential BM layer) were counted. Counting was performed in the narrow peritbular interstitium and avoided portions cut tangentionally and fibrotic areas.

4. The distance between the intercept point and the innermost PTCBM layer was defined as subendothelial space.

HCA was used to establish clinicopathologically distinct TxG subgroups based on the above-described ultrastructural parameters. The input ultrastructural variables for HCA were selected based on earlier studies that have demonstrated that reduced eGFR in nephrotic syndrome is due to reduction in the overall ultrafiltration coefficient (K_f) [81, 82]. K_f is the product of the hydraulic permeability of the glomerular capillary wall and the total capillary surface area. While calculating the actual K_f was beyond the scope of our study, we hypothesized that by using ultrastructural variables that influence the permeability of a given glomerular capillary wall component, an ultrastructurally distinct TxG subgroup with worse prognosis can be identified statistically. Therefore, EFg frequency, mean harmonic glomerular endothelial thickness, δ_{GBM}, and FS frequency were chosen for HCA of the TxG group.

Peritubular Capillary Basement Membrane Multilayering in Early and Advanced Transplant Glomerulopathy: Quantitative Parameters and Diagnostic Aspects

This retrospective study was performed at the Department of Pathology, University of Szeged and its patient population and that of the first study partially overlapped. Here, enrollment criteria included morphological signs of DSA-endothelium interaction in addition to TxG. Furthermore, the surveyed period was extended until 2014, and patients seropositive for HCV were excluded. Based on these modifications, fifty-seven patients were selected for this study.

We defined two study cohorts to explore the diagnostic utility of the different thresholds (permissive, intermediate and strict) for DSA-mediated PTCBMML and to examine what mean PTC_{CIRC} values are typical of early and fully developed chronic ABMR. The definition of mean PTC_{CIRC} was the same as in the previous study. The subgroup of mild TxG included cases with a Banff score of cg1a-b, while the subgroup of moderate-to-severe TxG consisted of patients with a Banff score of cg2-3. The difference between the cohorts for clinical, and demographic parameters, and for graft survival was tested. The capacity of the different PTCBMML thresholds to discriminate between cg1 *vs* cg2-3 were expressed using the sensitivity and the specificity of the thresholds for the cg2-3 lesion. An optimal cutoff value of PTC_{CIRC} for the same purpose was determined by performing a receiving operator characteristic (ROC) curve analysis [83].

Results

Morphologic Features and Clinical Impact of Arteritis Concurrent with Transplant Glomerulopathy

Demographic and Clinical Data

The median age of the study population was 44 years (IQR = 23). Thirty-two percent of the patients were female. Median time to biopsy from transplantation was 58 months (IQR = 67). At the time of the biopsy, two-third of the patients were in stage IV or V chronic kidney disease [84]. All but two recipients received a deceased donor kidney, and in all cases both donors and recipients were Caucasians. No ABO-incompatible transplantation was performed. 75 percent of the patients were on a calcineurin inhibitor (CNI)-based maintenance immunosuppressive regimen. One patient was tested for the presence of DSAs, the result was positive for class II HLA alloantibodies. The demographic and clinical characteristics in the two study groups at the time of the biopsy did not differ significantly.

Biopsy Findings in the Study Groups

Transplant glomerulopathy was identified by light and electron microscopy in 53 biopsies and exclusively by EM in 6 biopsies. In 16 biopsy samples TxG was accompanied by arteritis. Nine out of these 16 cases were C4d positive, six were C4d negative with at least moderate MVI, and one had no signs of activity. The arteritis lesion involved the intima of the interlobular arteries, and consisted of mononuclear cells with occasional foam cells. In 15 samples, the inflammatory cells were scattered throughout the fibrously thickened intima and were associated with severe (Figure 8) moderate or mild luminal narrowing in 10, four and one samples, respectively (cv_{mo} lesion).

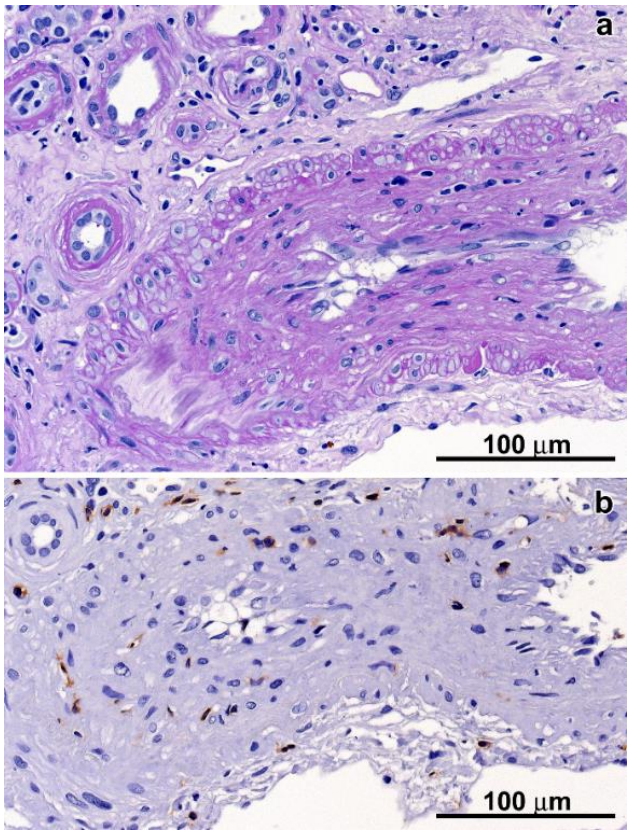

Figure 8. *Features of fibrosing intimal arteritis in adjacent sections. (a): Scattered mononuclear cells are located in the fibrously thickened intima; the vessel lumen is markedly narrowed. PAS, magnification x40. (b): the majority of the mononuclear cells proved to be T-lymphocytes. CD3 immunostain, 40x.*

The cell density within the inflamed intima was between 50-500 CD3+ cells/mm^2. In the biopsy of a patient with documented noncompliance, the infiltrate was also accompanied by insuded fibrinoid material. The mean ratio of involved arteries per biopsy was 62 percent.

The immunophenotyping of arteritis revealed the presence of CD3 positive, CD8/TIA-1 positive, and CD68 positive cells in 15, 10 and five cases, respectively. Only T-cells were found in 11 cases, while in five cases macrophages could also be identified. CD68+ cells were the dominant cell type in two cases. Five of the 10 samples with intimal cytotoxic T-cells displayed concurrent TCMR, and three of that 10 exhibited concurrent borderline changes and tubular HLA-DR expression. Biopsies with arteritis had significantly more severe interstitial inflammation (Table 1).

The grade of luminal narrowing was more severe in biopsies with cv_{mo} (median score = 3) than in biopsies with cv_{IF} or cv_{IFE} (median score = 1, $p < 0.001$). Forty-three patients did not show

Table 1. *Comparison of median values of Banff scores describing the severity of interstitial inflammation in the study groups.*

	TxG without arteritis (n = 43)	TxG with arteritis (n = 16)	*p-value*
i[a]	1	1.5	0.038
i-IF/TA[b]	1	1.5	0.027
ti[c]	1	2	0.018

[a]Interstitial infiltrate in the nonscarred cortex, [b]Interstitial infiltrate in the scarred cortex, [c]Interstitial infiltrate in the entire cortex

arteritis lesion. Eighteen of them were C4d positive, 22 cases showed at least moderate MVI without C4d positivity, and three cases were negative for both MVI and C4d. There was no significant difference for the distribution of coinciding pathologies between the study groups (Table 2).

Table 2. *Distribution of coinciding lesions in the index biopsies of the study groups (n of patients showing a particular lesion in each group are indicated).*

	TxG without arteritis (n = 43)	TxG with arteritis (n = 16)	p-value
T-cell mediated rejection	8	5	0.311
Borderline changes	13	6	0.755
Tubular HLA-DR positivity	18	11	0.242
Calcineurin inhibitor toxicity	16	6	1
Glomerulonephritis	4	4	0.194
HCV positivity	3	2	0.606

Statistical association of cv_{mo}, cv_{if}, and cv_{ife} with the Banff lesions

Luminal narrowing due to cv_{mo} correlated with the severity of interstitial inflammation in the scarred cortex ($r_S = 0.365$, $p = 0.005$) and total interstitial inflammation ($r_S = 0.352$; $p = 0.006$). PTCBMML showed association with cv_{if} ($r_S = 0.419$, $p = 0.001$). Intimal fibroelastosis did not correlate with other variables. HCA revealed three groups of the morphological alterations

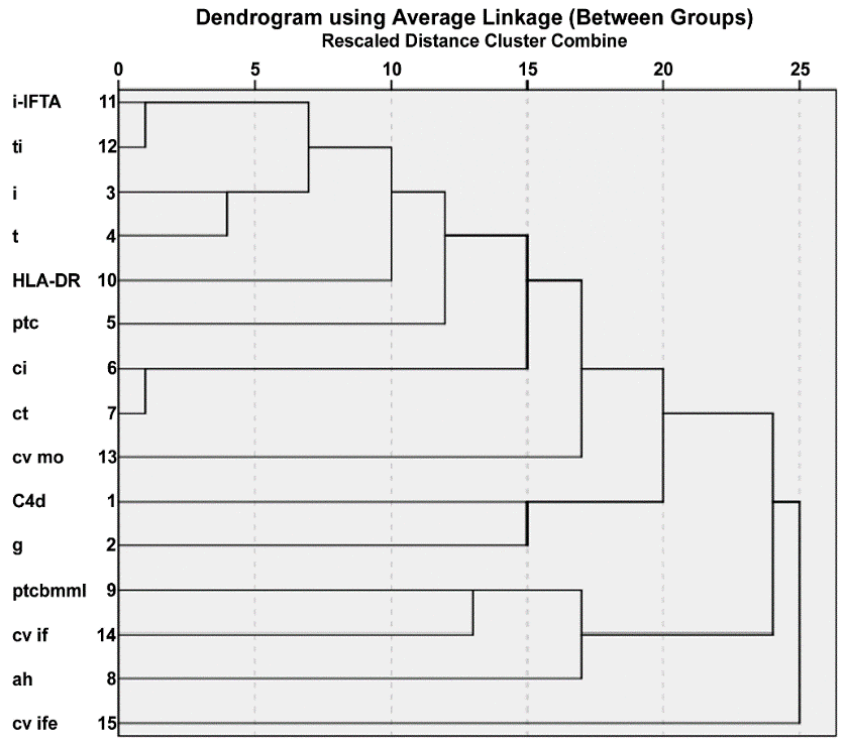

Figure 9. *Hierarchical cluster analysis diagram of the morphological variables. The first group comprised inflammation in scarred areas (i-IF/TA), total inflammation (ti), inflammatory infiltrate (i), tubulitis (t), tubular HLA-DR expression, peritubular capillaritis (ptc), interstitial fibrosis (ci), cvmo, C4d positivity, and glomerulitis (g). The second group consisted of peritubular capillary basement membrane multilayering (ptcbmml), cvif, cg and arteriolar hyalinosis (ah). Cvife did not group with other lesions.*

(Figure 9). The three chronic arterial changes clustered separately: while cv_{mo} was grouped with mostly acute lesions, cv_{if} was coupled with chronic vascular alterations, and cv_{ife} remained separate.

Post-biopsy management and graft survival

All 13 patients with a histological diagnosis of acute TCMR received steroid pulse therapy. In two cases with arteritis and concurrent acute TCMR, anti-thymocyte globulin and plasmapheresis were also administered. For the patients who had concurrent borderline changes, the immunosuppression was intensified. Different therapeutic approaches were applied in the cases of isolated arteritis: two patients received steroid pulse therapy, one patient participated in intensified immunosuppression, and two patients continued the same therapeutic regimen as in the pre-biopsy period.

The median duration of the post-biopsy follow-up was 20 months (IQR = 25.50). There was no significant difference for the means of eGFR between the TxG with *vs* without arteritis groups at the time of biopsy, as opposed to the eGFR measurements at three, six, and 12 months post-biopsy which differed significantly (Figure 10).

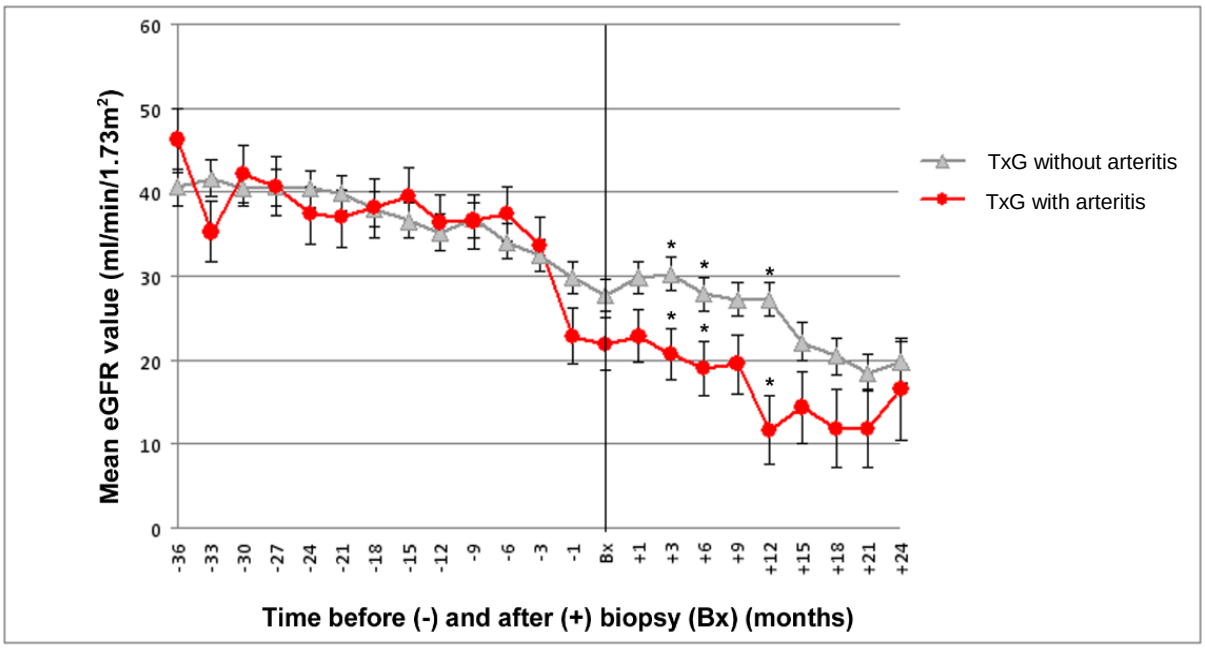

Figure 10. *Mean estimated glomerular filtration rates in the transplant glomerulopathy groups with vs without arteritis. The renal function in the former group was significantly worse than that in the latter at 3, 6 and 12 months post-biopsy (value pairs indicated by *).*

Forty-two graft failures were attributed to rejection. From among the 17 censored cases, nine patients died with a functioning allograft and three functioning grafts had been removed, in two patients due to sepsis, and in one patient because of massive bleeding after the biopsy puncture. The median graft survival of the patients with arteritis was 7.5 months [95 percent confidence interval (CI), 2 to 13], significantly lower than that of those without arteritis [29 months (95 percent CI, 17 to 41), p=0.001, Breslow method, Figure 11a)]. After the cases with glomerulonephritis had been excluded, the median graft survival in the arteritis group remained significantly worse [six months (95 percent CI, 2 to 10)] compared to patients without arteritis [32 months (95 percent CI, 22 to 42), p < 0.001]. In addition, the median graft survival was significantly lower for patients with arteritis [six months (95 percent CI, 2 to 10)] than for those non-arteritis patients who had TCMR [35 months (95 percent CI, 1 to 69), p=0.010]. Further, grafts with cv_{mo} had a worse median survival than grafts with cv_{IF}, or cv_{IFE} [7.5 months (95 percent CI, 3 to 12) *vs* 21 months (95 percent CI, 11 to 31) *vs* 35 months (95 percent CI, 21 to 49), respectively (p<0.001) (Figure 11b).

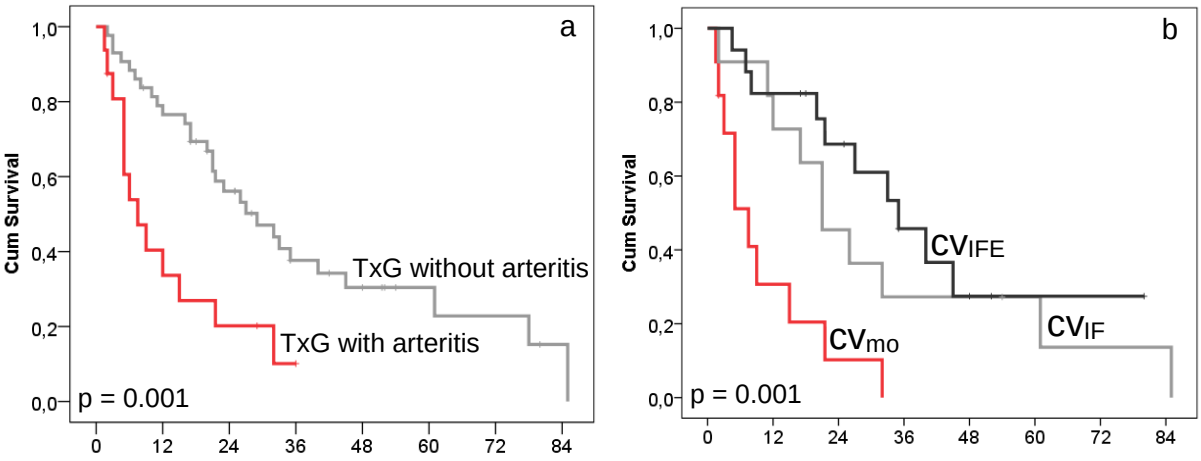

Figure 11. *Graft survival estimates: TxG with arteritis had a worse prognosis than TxG without arteritis: (a) all patients (n=59). Fibrosing intimal arteritis ($cv_{mo,}$ n = 15) has the worst prognosis compared to intimal fibrosis ($cv_{IF,}$ n =11) and intimal fibroelastosis ($cv_{IFE,}$ n = 20) (b).*

Quantitative Changes of the Renal Microvasculature in Transplant Glomerulopathy

Demographic and clinical characteristics of the TxG and the Protocol groups

There was no significant difference between the Protocol and the TxG groups for the main demographic, and serologic parameters (Table 3). Testing for DSA was performed in 60 percent of the TxG patients and 61 percent of those tested were positive. All but one patient in each group were on a CNI-based maintenance immunosuppressive regimen at the time of the biopsy. Median time-to-biopsy was significantly longer, while median eGFR was significantly lower in the TxG group relative to the protocols (Table 3). In addition, more than two-third of the TxG patients had severe proteinuria (as defined by Kidney Disease – Improving Global Outcomes initiative [85]), while none of them had in the protocol cohort (Table 3).

Histological features of the TxG and the Protocol group

Forty percent of the TxG patients met the histological criteria of C4d-positive chronic active ABMR as defined by the Banff 2015 classification [66]. Diffuse or focal C4d positivity was present in 12.5 percent and 27.5 percent of the cases, respectively. Forty-seven percent of the patients had the morphological requisites of chronic active C4d negative ABMR, while 13 percent of them did not show morphological signs of activity. Glomerular double contouring was mild (cg1b) in 13 cases, moderate (cg2) in 20, and severe (cg3) in 14 cases. Severe PTCBMML was present in nine percent of the cases.

In regards to the concurrent lesions, 22 TxG cases showed borderline changes while six had TCMR. On previous biopsies from the same allograft, 17 TxG patients were diagnosed with various severity of cell-mediated alloimmune response, seven with acute ABMR, two with acute pyelonephritis and seven with at least moderate interstitial fibrosis and tubular atrophy. The control group –by study design- showed only minor non-specific light microscopic changes.

Table 3. *Demographic data and clinical characteristics of the study groups at the time of the biopsy procedure. Pairwise comparison for each listed parameter was performed by Mann-Whitney U test, significant p-values are in bold.*

	Protocol (n=11)	**TxG[a] (n=47)**	***p*-value**
Donor female gender (n)	5	22	1.00
Donor age (years)	41 (20)[b]	41 (17)	0.76
Form of transplantation (n)			
living unrelated	1	3	1.00
living related	1	14	0.26
deceased donor	9	29	0.30
pancreas-kidney	0	1	1.00
Recipient female gender (n)	6	17	0.31
Recipient age (years)	45 (15)	50 (16)	0.85
Recipient race, non-black (n)	11	38	0.18
HLA mismatch (n)	3 (2)	4 (2)	0.06
Pre-transplant panel reactive antibodies (n of patients with >0 %)	1	22	**<0.005**
DSA[c] profile			
Patients only with Class I DSA (n)	n.a.[d]	4	n.a.
Patients only with Class II DSA (n)	n.a.	9	n.a.
Patients with Class I and II DSA (n)	n.a.	4	n.a.
No DSA was detected (n)	n.a.	11	n.a.
Class I DSA MFI[e]	n.a.	4215 (7038)	n.a.
Class II DSA MFI	n.a.	9392 (11343)	n.a.
Post-transplantation time (months)	10 (6)	54 (66)	**<0.005**
eGFR[f] level (ml/min/1.73 m^2)	75 (43)	33 (21)	**<0.005**
Urine Protein/Creatinine ratio (mg/g)	130 (50)	890 (1910)	**<0.005**

[a]Transplant glomerulopathy, [b]Interquartile ranges are in brackets, [c]Donor-specific antibody, [d]not applicable (DSA was not measured in normal protocol cases), [e]Mean fluorescent intensity, [f]Estimated glomerular filtration rate

Ultrastructural parameters of the protocol biopsies were similar to the findings reported in previous studies on normal, native kidney specimens [82, 86, 87]. The TxG group showed statistically significant changes relative to the Protocols in regards to all three components of the filtration barrier and the PTCs (Table 4).

Table 4. *Medians of the ultrastructural parameters of the study groups. Mann-Whitney U test was used for pairwise comparisons, all tests proved to be significant ($p < 0.0005$, interquartile ranges are in brackets).*

	Protocol	**TxG**
Mean harmonic glomerular basement membrane thickness (nm)	319 (90)	890 (520)
Filtration slit frequency (unit/mm)	1490 (280)	1110 (410)
Endothelial fenestrae frequency, glomerulus (unit/mm)	2160 (120)	720 (640)
Mean harmonic endothelial thickness, glomerulus (nm)	100 (20)	220 (160)
Peritubular capillary basement membrane multilayering (n of layers)	1.1 (0.44)	2.8 (1.31)
Endothelial fenestrae frequency, peritubular capillary (unit/mm)	1390 (160)	230 (210)
Mean harmonic peritubular basement membrane thickness (nm)	148 (30)	424 (110)
Mean harmonic endothelial thickness, peritubular capillary (nm)	102 (40)	360 (160)

Correlations between the ultrastructural alterations and the laboratory/serological parameters

Estimated GFR showed the strongest correlation with mean harmonic endothelial thickness in the PTCs, while the strongest association of urine protein/creatinine ratio was with δ_{GBM} (Table 5).

Table 5. *Rho values of Spearman's rank correlation tests between ultrastructural variables and laboratory-serological parameters (p-value for each r_S is shown below the corresponding correlation coefficient*).

	δ_{GBM}[a]	EF[b] frequency glom.[c]	δ_{END}[d] glom.	FS[e] frequency	δ_{PTCBM}[f]	EF frequency PTC[g]	δ_{END} PTC
eGFR	-0.565 <0.001	0.355 0.006	-0.467 <0.001	0.417 0.001	-0.499 <0.005	0.641 <0.001	-0.713 <0.001
Urine protein/ creatinine ratio	0.626 <0.001	-0.527 <0.001	0.56 <0.001	-0.347 0.008	0.416 0.001	-0.392 0.002	0.569 <0.001

[a]mean harmonic GBM thickness, [b]endothelial fenestra, [c]glomerulus, [d]mean harmonic endothelial thickness, [e]filtration slit, [f]mean peritubular capillary basement membrane thickness, [g]peritbular capillary

Associations between serological and ultrastructural parameters were also tested in a subgroup of patients, where DSA data were available (n = 28). Patients tested negatively for DSA had significantly lower PTC endothelial thickness (270 nm, IQR = 170) than those with Class II DSA in combination with Class I or alone (350 nm, IQR = 200, p = 0.047). In addition, PTC EF frequency was higher in DSA negative patients (310 unit/1 mm PTC, IQR = 510) compared to the Class II DSA positive group (220 unit/1 mm PTC, IQR = 210, p = 0.035).

Hierachical Cluster Analysis of the Transplant Glomerulopathy Patients

Hierarchical cluster analysis based on EF_g frequency, glomerular endothelial width, δ_{GBM}, and FS frequency separated the TxG patients into two subgroups (Figure 12).

Figure 12. *Hierarchical cluster analysis of transplant glomerulopathy patients. Two subgroups (Cluster 1 and Cluster 2) could be identified based on glomerular ultrastructural parameters. Patients' individual study IDs are shown on the x-axis.*

There was a significant difference for the glomerular ultrastructural parameters and PTC endothelial thickness between the two subgroups: in summary, "Cluster 1" (n = 27) was characterized by more subtle ultrastructural alterations, while "Cluster 2" (n = 20) was more deviant from the Protocol group's measurements (Table 6).

Table 6. *Median values and interquartile ranges of selected ultrastructural parameters in the transplant glomerulopathy subgroups identified by hierarchical cluster analysis. Pairwise comparisons were performed by Mann-Whitney U test, significant p-values are in bold.*

	TxG Cluster 1	**TxG Cluster 2**	p-value
Mean harmonic GBM[a] thickness nm (nm)	660 (310)	1295 (380)	**<0.0005**
Filtration slit frequency (unit/mm)	1020 (670)	470 (340)	**<0.0005**
Endothelial fenestrae frequency, glomerulus (unit/mm)	170 (70)	320 (120)	**<0.0005**
Mean harmonic endothelial thickness, glomerulus (nm)	1160 (220)	860 (420)	**0.002**
Mean harmonic endothelial thickness, PTC[b] (nm)	330 (160)	400 (200)	**0.03**

[a]glomerular basement membrane, [b]peritubular capillary

The light microscopic characteristics of the TxG subgroups were comparable (Table 7), as well as the basic demographic, and serologic data (Table 8). Renal function parameters in "Cluster 2" were inferior relative to "Cluster 1" at the time of the diagnosis and at two years after the biopsy procedure (Table 8).

Table 7. *Histological characteristics of the transplant glomerulopathy subgroups identified by hierarchical cluster analysis: median values of Banff scores and coinciding lesions. Interquartile ranges are in brackets, no significant p-values were found.*

	TxG Cluster 1 (n=27)	**TxG Cluster 2 (n=20)**	*p-value*
Glomerulitis (g)	2 (2)	2 (1.75)	0.644
Peritbular capillaritis (ptc)	1 (2)	2 (1.75)	0.680
Interstitial infiltrates (i)	1 (1)	1 (1.75)	0.872
Tubulitis (t)	1 (1)	1 (1)	0.830
Arteritis (v)	0 (0)	0 (0)	not applicable
Transplant glomerulopathy (cg)	2 (1)	2 (1.75)	0.164
Interstitial fibrosis (ci)	1 (1)	2 (1.75)	0.137
Tubular atrophy (ct)	1 (1)	1.5 (1)	0.681
Arterial intimal fibrosis (cv)	1 (2)	1 (1)	0.166
Arteriolar hyalinosis (ah)	1 (3)	1 (2.50)	0.867
Features suggestive of chronic cal-cineurin inhibitor toxicity (n)	2	1	0.613
Total inflammatory infiltrate (ti)	1 (1)	1 (1)	0.889
C4d positivity (n)	8	11	0.080
Coinciding cell-mediated alloimmune injury in the index (first TxG) biopsy			
Borderline changes (n)	10	12	0.119
Acute cellular rejection (n)	5	2	0.682

Table 8. *Demographic data, clinical characteristics and basic serological parameters of the transplant glomerulopathy subgroups identified by hierarchical cluster analysis, significant p-values are in bold, interquartile ranges are in brackets.*

	TxG[a] Cluster 1 (n = 27)	**TxG Cluster 2 (n = 20)**	*p-value*
Donor female gender (n)	13	9	1.000
Donor age (years)	42 (11)	34.50 (16.50)	0.084
Recipient female gender (n)	10	7	1.000
Recipient age (years)	50 (28)	49.50 (11.50)	0.846
Recipient race, black (n)	7	2	0.266
Pre-transplant panel reactive antibodies (%)	8	14	0.069
DSAd[b] profile			
Patients only with Class I DSA (n)	1	3	0.139
Patients only with Class II DSA (n)	6	3	1.000
Patients with Class I and II DSA (n)	3	1	1.000
No DSA was detected (n)	7	4	1.000
Class I DSA MFI[c]	4214.8 (6477.6)	4738.50 (10388.2)	1.000
Class II DSA MFI	12462 (12007.8)	8169.25 (9676.8)	0.604
Post-transplantation time (months)	50 (67)	67 (87)	0.156
eGFR[d] level (ml/min/1.73 m^2)	40 (23)	27.50 (15)	**0.044**
eGFR level at the post-biopsy 24th month[e]	39.5 (20.5)	29 (16)	**0.021**
Proteinuria			
Urine Protein/Creatinine ratio (mg/g)	800 (1610)	1275 (2992.5)	**0.028**
>3500 mg/g (n)	0	6	**0.004**

[a]Transplant glomerulopathy, [b]Donor-specific antibody, [c]Mean fluorescent intensity, [d]Estimated glomerular filtration rate, [e]Only those patients were considered, whose kidney function was > 15 (ml/min/1.73 m2) at 24 month postbiopsy

Therapeutic interventions after the index biopsy procedure were also compared. Intravenous immunoglobulin (alone or in combination with anti-CD20 monoclonal antibody) was given to similar proportion of the patients in both clusters. Plasmapheresis completed the anti-rejection treatment for three patients in “Cluster 1” and a single patient in “Cluster 2”. Patients with varying levels of cellular alloimmune injury in their index biopsy sample also underwent steroid pulse therapy. Kaplan-Meier curves of the TxG subgroups are shown in Figure 13. Cumulative survival proportion for “Cluster 1” did not dip below 0.5 by the end of the follow-up period, unlike that of “Cluster 2” patients who had a median graft survival rate of 25 months (95 percent

CI, 4 to 46) (Figure 13a). We also analyzed the prognostic relevance of the "Cluster 1" *vs* "Cluster 2" distinction by controlling for interstitial fibrosis: each cluster was further split into three cohorts based on the involvement of the cortex by interstitial fibrosis (mild: < 25 percent, moderate: 25 to 50 percent, and severe: > 50 percent of the cortical area).

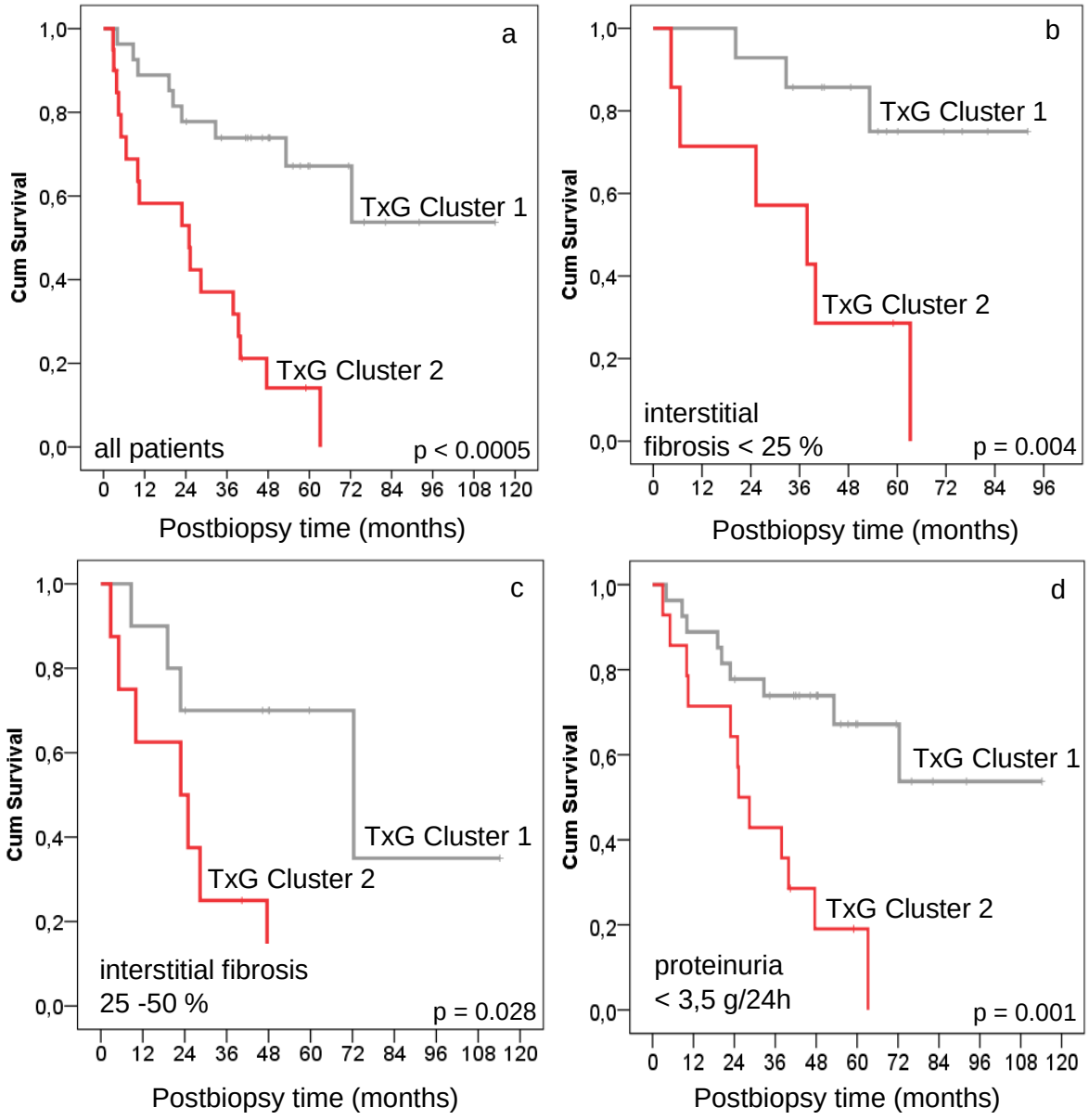

Figure 13. *Kaplan-Meier curves of the transplant glomerulopathy subgroups identified by hierarchical cluster analysis. Cluster 2 had lower graft survival rate relative to Cluster 1 (Panel a). On Panel b, and c, pairwise comparisons between Cluster 1 and Cluster 2 patients with different levels of chronicity are shown. Panel d, shows the graft survival rates of Cluster 1 and Cluster 2 after patients with nephrotic range proteinuria were excluded.*

Next, “Cluster 1” and “Cluster 2” patients that belonged to a given “chronicity” cohort were compared pairwise. The difference in graft survival distributions remained significant in the mild and moderate interstitial fibrosis cohorts (Figure 13 b and c). In the mild cohort, only three out of the 14 “Cluster 1” patients lost their allograft within the follow-up period, while “Cluster 2” patients (n = 7) had a median graft survival rate of 38 months (95 percent CI, 6 to 70). In the moderate cohort, “Cluster 1” patients’ (n = 10) median graft survival rate was 72 months (95 percent CI, 1 to 144), higher than that of “Cluster 2” patients [n = 8; median graft survival rate = 23 months (95 percent CI, 2 to 44)]. Survival distributions for “Cluster 1” and “Cluster 2” patients in the severe interstitial fibrosis cohort were not statistically significantly different. In addition, we also analyzed the two clusters after excluding patients with nephrotic range proteinuria (n = 6, Figure 13 d). The difference between the survival rates of the two clusters remained significant, Cluster 2 patients’ median graft survival rate was 25 months (95 percent CI, 19 to 32), while that of Cluster 1 did not change (since all excluded patients belonged to Cluster 2).

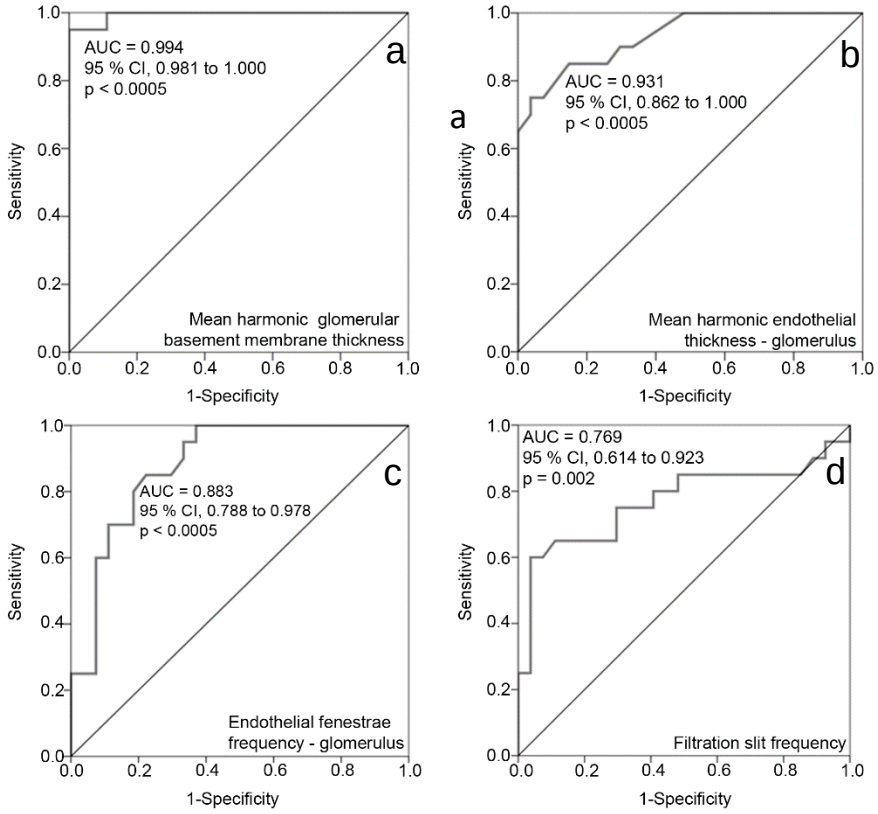

Lastly, ROC-curve analysis was used to test the ability of each ultrastructural parameter in the HCA model to identify the TxG clusters (Figure 14). The most discriminative marker was δ_{GBM}. A threshold of 925 nm had the capacity to separate “Cluster 1” from “Cluster 2” with a 100 percent sensitivity and 95 percent specificity.

Figure 14. *Receiving operator characteristics curve analysis of ultrastructural parameters used in hierarchical clustering for transplant glomerulopathy patients. Mean harmonic glomerular basement membrane thickness stood out as the variable with the highest specificity and sensitivity to the pattern of severe glomerular alterations (a).*

Peritubular Capillary Basement Membrane Multilayering in Early and Advanced Transplant Glomerulopathy: Quantitative Parameters and Diagnostic Aspects

Demographic, Serologic and Clinial Features of Patients with Mild *vs* Moderate-to-severe TxG

There was no significant difference for gender, age, HLA-mismatch, PRA titer, and maintenance immunosuppression strategy between patients with mild (n = 15) and moderate-to-severe TxG (n = 42) (Table 9). All recipients and donors in both groups were Caucasians and all transplantations were ABO group compatible. In each group, all but one recipient received a deceased donor kidney. DSAs against HLA class I/II antigens were demonstrated in the nine tested recipients (Table 9). Patients with moderate-to-severe TxG had significantly lower eGFR, and more severe proteinuria than those with mild TxG at the time of biopsy (Table 9). The elapsed time from transplantation to biopsy was significantly shorter in the subgroup of mild TxG (Table 9). In addition, patients with moderate-to-severe TxG had a significantly lower graft survival than that of patients with mild TxG (Figure 15).

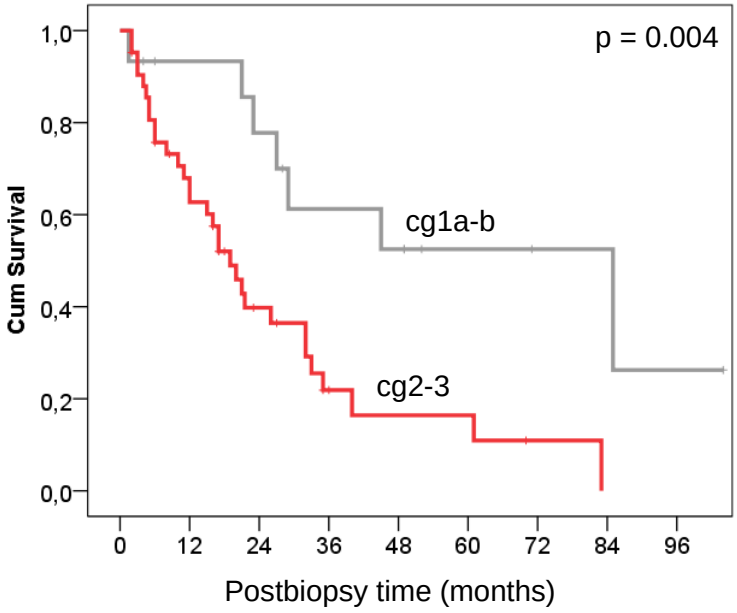

Figure 15. *Patients with mild TxG had a significantly longer graft survival [85 months (95 % CI, 23 to 147)] than patients with moderate to severe TxG, [19 months (95 % CI, 14 to 24)]*

Table 9. *Demographic data and clinical characteristics of the recipients at the time of the biopsy procedure. Significant p-values are in bold, interquartile ranges are in brackets.*

	cg1 (n=15)	cg2-3 (n=42)	*p*-value
Recipient female gender (n)	3/15	14/42	0.513
Recipient age (years)	43 (22.00)	43.50 (20.50)	0.993
Previous Tx[a] (n patients with >1 Tx)	3	5	0.422
Result of HLA matching (n of patients)			
no HLA mismatch	2	17	0.065
at least 1 or more HLA mismatch	13	25	
Panel reactive antibodies (n of patients)			
Not detected	9	21	0.8
At least 1 %	3	3	
No data	3	18	
Post-transplantation time (months)	42 (46)	71 (70.5)	**0.007**
Maintenance immunosuppression (n of patients)			
Calcineurin inhibitor	14	32	0.256
Mycophenolate mofetil	11	35	0.455
Steroid	11	23	0.239
Mechanistic target of rapamycin inhibitor	4	12	1
eGFR[b] level (ml/min/1.73 m^2)	30.6	19.7 (13.10)	**0.009**
Class I DSA[c] MFI[d]	3351 (2097)	10556.5 (8841)	n.a.[e]
Class II DSA MFI	2826 (11340)	1797 (6389)	n.a.
Proteinuria			
Daily amount of proteinuria (g/24h)	0.97 (1.95)	2.73 (5.36)	**0.009**
< 3.5 g/24 h (n of patients)	14	30	0.15
≥ 3.5 g/24 h (n of patients)	1	12	

[a]Transplantation, [b]Estimated glomerular filtration rate, [c]Donor-specific antibody, [d]Mean fluorescent intensity value, [e]Not applicable (because of the limited number of examined patients, significance was not tested)

Histological Characteristics of the Study Groups

Out of the 15 mild TxG lesions, four showed glomerular double contouring exclusively by EM. Eleven case was diagnosed as moderate TxG, while severe GBM reduplication could be observed in 31 cases. Severe PTCBMML diagnostic of chronic ABMR based on the Banff 2013 [65] classification was present in 40 percent of the cases. C4d negative and positive cases were

present in almost equal proportion in the study groups (Table 10). In total, 28 index biopsies did not display C4d positivity. However, seven out of these patients had a previous biopsy with at least focal C4d signal, while eight out of them had tissue specimens subsequent to the index biopsy with C4d positivity. In regards to the concurrent lesions in the index biopsy samples, no significant difference was found between the two groups (Table 10).

Table 10. *Histological characteristics of the study groups.*

	cg 1 (n=15)	cg 2-3 (n=42)	*p-value*
C4d positive chronic active ABMR	8	21	1.000
C4d negative chronic active ABMR	7	21	1.000
Coinciding lesions in the index (first TxG) biopsy			
Borderline changes	4/15	12/42	1.000
T-cell mediated rejection	3/15	1/42	1.000
IgA glomerulonephritis	1/15	3/42	1.000
Severe arteriolar hyalinosis	6/15	19/42	0.771

Association of PTC_{CIRC} with Other Morphological Lesions

We analyzed a median of 16 capillaries/case (IQR = 3) and found that PTC_{CIRC} was significantly higher in moderate-to-severe TxG (4.5 layers, IQR = 2.03), than in mild TxG (2.6 layers, IQR = 1.56, $p < 0.0001$), as well as in patients with at least moderate glomerulitis (3.82 layers, IQR = 1.93) relative to those with mild glomerulitis (2.38 layers, IQR = 1.63). At least moderate peritubular capillaritis, C4d positivity and presence of TCMR did not have a similar association with PTC_{CIRC}.

The Effect of Sample Size on Establishing the Diagnosis of DSA-mediated PTCBMML

We determined the proportion of those cases that would satisfy the different PTCBMML thresholds if only 10 PTCs were sampled per case (i.e. the sensitivity of measuring 10 PTCs relative to the *de facto* measured number of PTCs). With the strict criterion we found this proportion to be 70 percent, while in the case of intermediate and permissive criteria the

concordance was 79 percent and 92 percent. We also studied the ability of PTC_{CIRC} -calculated after 10 PTCs had been sampled- to predict the PTC_{CIRC} based on all sampled PTCs. By applying linear regression, we were able to build a significant regression model represented by $PTC_{CIRC} = 0.215 + 0.969 \times PTC_{CIRC,10}$ ($p < 0.001$), where PTC_{CIRC} is the value based on all measured PTCs while $PTC_{CIRC,10}$ is the value based on the first 10 measured PTCs.

Capacity of PTCBMML Thresholds to Discriminate Between Mild and Moderate-to-severe TxG

The permissive criterion had a specificity of 73 percent and a sensitivity of 81 percent for cg2-3. A higher specificity (87 percent), and a lower sensitivity (64 percent) were measured with the intermediate criterion; the strict criterion displayed the highest specificity (93 percent), but the lowest sensitivity (52 percent). With a ROC-curve analysis, a cutoff point of 3 BM layers/PTC was found to have a sensitivity and specificity similar to those of the permissive criterion [83 percent and 73 percent, respectively (AUC = 0.838, 95 percent CI = 0.731-0.945, $p < 0.0001$)]. The PTC_{CIRC} value that matched the strict threshold was 4.0 layers (with a specificity of 93 percent and sensitivity of 57 percent). A single PTCBMML cutoff that represents the intermediate threshold could not be given, as it involved two thresholds (one PTC with equal to or more than seven layers or three PTCs with five to six layers) that could not be translated into a single PTC_{CIRC} value. Next, we calculated the proportions of the cases in the mild and moderate-to-severe TxG subgroups that would meet the three different PTCBMML thresholds. In mild TxG, 27 percent of the cases met the permissive criterion, 13 percent met the intermediate criterion and only 7 percent had severe PTCBMML (strict criterion). The corresponding values in moderate-to-severe TxG were 81 percent (permissive), 64 percent (intermediate) and 52 percent (strict).

Prognostic Value of PTCBMML Thresholds and $PTC_{CIRC} \geq 3$ in Post-biopsy Graft Survival

Patients were divided into subgroup pairs based on each threshold and the median graft survival rates were compared pairwise (Figure 15). Patients who met the permissive citerion for

PTCBMML had a lower median graft survival rate [19 months (95 percent CI, 15 to 23)] than those who did not (40 months (95 percent CI, 19 to 61) (Figure 16a). The PTC_{CIRC} value that matched the permissive criterion (3 layers) resulted in subgroups with identical graft survival rates (Figure 15b). The intermediate criterion and the strict criterion, however, did not split the TxG patients into prognostically different cohorts (Figure 15c and d).

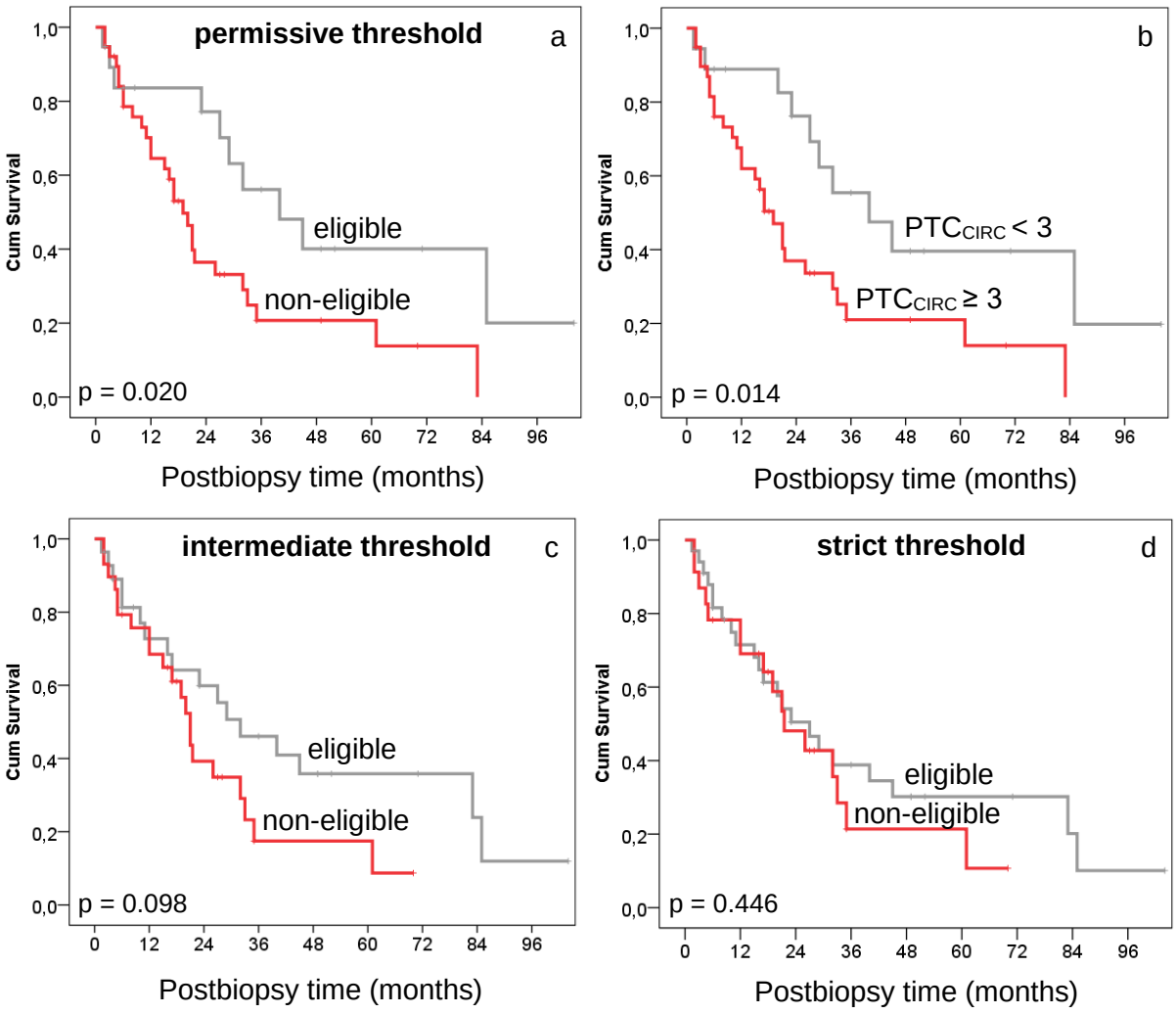

Figure 16. *Graft survival rates of TxG subgroups defined by different PTCBMML thresholds. Both the permissive threshold and* $PTC_{CIRC} \geq 3$ *defined subgroups with significantly different median graft survival rates [(a) and (b) panels, respectively). In contrast, if patients were dichotomized based on the intermediate or strict criteria for PTCBMML, no prognostically different subgroups were formed [32 months (95 percent CI, 14 to 50) vs 21 months (95 percent CI, 18 to 24)] (c); 27 months (95 percent CI, 16 to 38) vs 21.50 months (95 percent CI, 12 to 31) (d)].*

Discussion

Morphologic Features and Clinical Impact of Arteritis Concurrent with Transplant Glomerulopathy

In this study, 59 consecutive indication biopsies were analyzed to explore the clinicopathologic relevance of arteritis in patients with TxG. Although DSA data were available only in one patient, the additional biopsy findings supported the diagnosis of chronic active ABMR in 93 percent of the cases. Seven percent of the biopsy samples did not show activity that may indicate the cessation of alloantibody production prior to the biopsy procedure. The prevalence of arteritis was 27 percent (16/59).

The 'Banff' chronic vascular lesion was categorized in each case as intimal fibrosis (cv_{IF}), fibrosing intimal arteritis (cv_{mo}), or intimal fibroelastosis (cv_{IFE}). Our statistical tests (Spearman's correlation, HCA) connected these morphologic entities with different groups of histological variables. Fibrosing intimal arteritis correlated/was clustered mainly with inflammatory lesions, confirming the notion that it is an active process. In contrast, cv_{IF}, along with TxG and PTCBMML formed another group, emphasizing the chronic nature of these injuries. As opposed to the former two, cv_{IFE} did not have statistical association with other morphological lesions characteristic of the alloimune response that reflects the fact that this lesion is due to ageing and/or hypertension.

The intimal inflammatory infiltrate showed cytotoxic T-cells in two-third of the cases and was often accompanied by TCMR of varying severity, suggesting that T-cell-mediated mechanisms may have played a role in the evolution of cv_{mo} in certain cases. However, we also found 5 cv_{mo} cases with CD68+ cells (most likely macrophages) in the fibrotic intima. While four of them showed also concurrent TCMR, the presence of these cells may have been an indication of complement-mediated chemotaxis, a pathogenetic mechanism of chronic ABMR [41]. Based on these findings the precise separation of the etiological role of the two alloimmune pathways in cv_{mo} is not always feasible, and both cellular and antibody-mediated mechanisms can contribute to the development of this lesion.

The arteritis lesion exerted a strong negative effect on post-biopsy renal function and graft survival even after adjusting for the confounding effect of cases with glomerulonephritis. A possible explanation is that severe luminal narrowing was detected in more than two-third of the arteritis group. Another factor that might account for the worse survival of the patients with this lesion is the significantly higher inflammatory load that is a known negative prognostic factor [88] in renal transplant biopsies. The graft survival in patients with arteritis was also shorter than in patients with TCMR, which indicates that late-onset TCMR can be controlled more effectively than arteritis that significantly worsens graft outcomes in patients who developed TxG.

Quantitative Changes of the Renal Microvasculature in Transplant Glomerulopathy

We analyzed 47 renal transplant biopsies with TxG secondary to chronic active ABMR, and 11, normal, protocol cases as controls. Our aim was to quantitatively characterize the chronic ABMR-associated ultrastructural changes of the renal microvasculature, and to explore the clinical relevance of these alterations. In accordance with the literature [35], our TxG cohort was heterogeneous for morphologic activity and presence of DSAs: while 16 out of the 47 TxG samples met all Banff 2013 criteria for cABMR [65], 26 had either DSA positivity or morphologic activity but not both. In addition, five cases showed neither DSA nor morphologic activity.

First, we compared the ultrastructural changes seen in our TxG cohort to normal protocol biopsies. We found that TxG patients showed major remodeling in both compartments of the renal microcirculation similarly to the previous report by Wavamunno *et al* [56]. Next, we studied the associations between the ultrastructural and laboratory parameters. We were able to show that the presence of Class II DSAs are associated with more severe PTC endothelial changes relative to that in those TxG subjects with no DSA. In addition, among the renal function parameters, eGFR showed the strongest negative correlation with PTC mean harmonic

endothelial thickness. These findings align well with reports on class II DSAs being a negative prognostic factor in chronic ABMR [38-40].

Our results also contribute to the ongoing debate about the diagnostic utility of PTCBMML in chronic active ABMR. The Banff 2013 classification adopted severe PTCBMML as a morphologic evidence of chronic antibody-mediated allograft injury. Although this cut-off is highly specific we found that its sensitivity in TxG patients is low. Furthermore, PTC_{CIRC} clearly showed the involvement of PTCs in patients with TxG compared to the protocol subjects. This finding along with the conclusions of other studies [73, 74, 89], emphasizes the need for a lower threshold for CABMR-induced PTCBMML to facilitate early diagnosis of the condition.

Based on the ultrastructural model of glomerular filtration [81] we were able to separate TxG patients into two prognostically different subgroups. Severe glomerular endothelial swelling, almost complete loss of fenestration, marked GBM thickening, and extensive foot process effacement characterized the patients with worse prognosis. We found that the cut-off of 925 nm of δ_{GBM} can identify this TxG subgroup with 100 percent sensitivity and 95 percent specificity.

Testing whether GBM thickness is an independent risk factor for allograft loss in a Cox-regression model was not statistically feasible due to the TxG cohort size and represents a limitation of our study. However, the ultrastructural distinction between the TxG clusters remained prognostic in the mild and moderate fibrosis cohorts after stratification for interstitial fibrosis, a major morphologic determinant of renal allograft survival [90]. In addition, after excluding patients with nephrotic range proteinuria (who all belonged to the TxG cohort with worse prognosis), the cohort retained its inferior graft survival rate. These data collectively suggest that the ultrastructural alterations can contribute to graft survival prognostication even at a stage when the TxG lesion already can be detected by light microscopy but patients yet to develop severe interstitial fibrosis, and electron microscopic metrics are able to identify a broader population at risk of graft loss than nephrotic range proteinuria alone.

Peritubular Capillary Basement Membrane Multilayering in Early and Advanced Transplant Glomerulopathy: Quantitative Parameters and Diagnostic Aspects

Here, we examined the status of PTCBMML in a series of 57 TxG cases. Our aim was to test the ability of the various PTCBMML thresholds and PTC_{circ} to differentiate early from advanced chronic AMBR and to explore their further possible clinical relevance. Due to the retrospective nature of the study, the DSA data were incomplete. Complement 4d positivity with or without MVI was found in 29 index biopsies, while MVI only was found in 28 samples. In total, 81 percent of our study population had either C4d positivity (including the index, previous, and follow-up biopsies) or DSAs at the time of the index biopsy, or both. These evidence suggest that ABMR was the driving force behind the development of glomerular double contours in our patient population.

We found that based on the clinical and laboratory parameters mild TxG represented early chronic ABMR, while moderate-to-severe TxG indicated a late and advanced manifestation of the process. In mild TxG, the permissive threshold for DSA-induced PTCBMML was noted in 26 percent, the intermediate in 13 percent, and the strict in only 6 percent of the cases. In addition, the permissive and the intermediate threshold separated moderate-to-severe TxG cases from mild TxG cases with a good sensitivity and specificity. In contrast, the strict threshold's had poor sensitivity but excellent specificity for moderate-to-severe TxG. These data collectively suggest that the strict threshold represent advanced ABMR, and are in accordance with the findings of Liapis *et al*. [69]

We studied the impact of sample size on establishing the diagnosis of ABMR-induced PTCBMML. We found that sampling of 10 capillaries resulted in a significant underdiagnosis of the lesion if it was defined by the strict threshold. In contrast, results obtained using the permissive criterion had a good concordance regardless of sample size. In conclusion, the permissive threshold allows the pathologist to reduce the time spent on the ultrastructural analysis of each specimen by examining only 10 PTC without risking to miss a significant number of cases.

In regards to the statistical connection between the Banff morphological variables and PTCBMML, severe glomerulitis was associated with higher scores of PTC_{CIRC}, indicating that ongoing inflammation in the microvasculature results in more severe chronic changes.

We also analyzed the prognostic utility of the PTC_{CIRC} value and the different PTCBMML thresholds, and only the permissive criterion/PTCcirc $\geq$ 3.0 proved to be prognostically relevant. Whether this effect is independent of the severity/presence of other morphological, clinical, and serological variables could not be assessed because of the limited number of patients. Nevertheless, since PTCcirc is a quantitative variable, its prognostic relevance is worth further studies in a larger patient population.

The results of the present study and those of two previous ones [73, 74] taken together suggest that the determination of PTC_{CIRC} values may be a better approach for the verification of early chronic ABMR-induced kidney injury than a search for the most severely laminated PTC profiles. In our study, the subgroup of mild TxG was characterized by a median PTC_{CIRC} of 2.6 BM layers, and the moderate-to-severe TxG subgroup by a significantly higher value of 4.5 layers. Since a mean PTCBM count greater than 2.5 layers preceded and predicted the development of TxG in the elegant study of de Kort *et al*. [74], and $PTC_{CIRC} \geq 3$ in the present study indicated a worse graft survival rate for patients with TxG, a PTC_{CIRC} value between 2.6 and 3 layers appears to represent a transitional range that indicates subclinical, ongoing ABMR in the renal microvascular bed, if non-alloimmune causes of PTCBMML are excluded clinicopathologically. The PTCcirc values are consistent, regardless whether 10 or more PTCs are sampled, which further supports the use of the mean PTCBM count as a tool for the evaluation of PTC involvement in chronic active ABMR.

Summary

In the work presented here, we explored the clinical relevance and morphological characteristics of macro-, and microvascular lesions associated with TxG the cardinal phenotype of chronic ABMR. Our reason to study the vascular alterations was that the morphological integrity of the renal vasculature is key in maintaining renal function. Although glomerular double contours are not specific to ABMR, our strict clinicopathological enrollment criteria, and detailed diagnostic workup by light, IF, and electron microscopy ensured that our study cases represented chronic ABMR-related injury.

In our first paper we examined the chronic arterial changes associated with TxG and found that fibrosing intimal arteritis worsened graft outcome. Its pathomechanism probably involved both arms of the alloimmune response and it was frequently associated with increased inflammatory load in the renal cortex that most likely also contributed to premature graft loss.

In our subsequent study, we focused on the microvascular alterations and showed that GBM thickening positively correlated with urine protein/creatinine ratio and a cut-off of 925 nm of δ_{GBM} identified a TxG subgroup with worse renal survival. This cutoff could capture those patients who, despite having a light microscopically apparent lesion, could still expect a significantly less steep survival curve. In addition to renal graft survival prognostication, δ_{GBM} may serve as a highly reproducible and sensitive surrogate biomarker for response-to-treatment in future drug studies.

Lastly, we studied PTCBMML associated with TxG. Based on our findings the current ("strict") threshold for DSA-induced PTCBMML could not facilitate the early detection of chronic ABMR since it was mainly present in cases where glomerular double contours were already obvious by light microscopy and a further ultrastructural examination for diagnostic purposes was unnecessary. In addition, this threshold also failed to demonstrate any prognostic value in patients with TxG. Based on these findings we recommend using the permissive criterion/PTCcirc $\geq$ 3.0 to diagnose DSA-mediated PTCBMML, because it represents the earliest, prognostically relevant morphologic manifestation of chronicity due to ABMR in an

appropriate clinicopathologic context (e.g. DSAs/C4d positivity/at least moderate microvascular inflammation).

In summary, chronic ABMR remains a major challenge that needs to be overcome to prolong long-term renal graft survival. Our findings prove that the detailed examination of the morphological changes in the renal vasculature can contribute to these ongoing efforts by identifying prognostic markers and refining diagnostic criteria that help to define a patient population which can benefit the most from the current therapeutic options.

References

1. Wolfe RA, Ashby VB, Milford EL, et al. Comparison of mortality in all patients on dialysis, patients on dialysis awaiting transplantation, and recipients of a first cadaveric transplant. *N Engl J Med.* 1999; 341: 1725-1730.

2. Ortiz F, Aronen P, Koskinen PK, Malmström RK, et al. Health-related quality of life after kidney transplantation: who benefits the most? *Transpl Int.* 2014; 27: 1143-1151.

3. de Wit GA, Ramsteijn PG, de Charro FT, et al. Economic evaluation of end stage renal disease treatment. *Health Policy.* 1998; 44: 215-232.

4. Valenzuela NM, Reed EF. Antibody-mediated rejection across solid organ transplants: Manifestations, mechanisms, and therapies. (Review Series: Transplantation). *J Clin Invest*. 2017; 127: 2492-2504.

5. Bhalla V, Nast CC, Stollenwerk N, et al. Recurrent and de novo diabetic nephropathy in renal allografts. *Transplantation.* 2003; 15: 66-71.

6. Denton MD, Singh AK. Recurrent and de novo glomerulonephritis in the renal allograft *Sem Nephrol*. 2000; 20: 164-175.

7. El-Zoghby ZM, Stegall MD, Lager DJ, et al. Identifying specific causes of kidney allograft loss. *Am J Transplant.* 2009; 9: 527-535.

8. Denton MD, Magee CC, Sayegh MH. Immunosuppressive strategies in transplantation. *Lancet*. 1999; 353: 1083-1091.

9. Chan L, Gaston R, Hariharan S. Evolution of immunosuppression and continued importance of acute rejection in renal transplantation. *Am J Kidney Dis*. 2001; 38 (6 Suppl 6): S2-9.

10. Kahan BD. Cyclosporine. *N Engl J Med.* 1989; 321: 1725-1738.

11. Groth CG, Bäckman L, Morales JM, et al. Sirolimus (rapamycin)-based therapy in human renal transplantation: Similar efficacy and different toxicity compared with cyclosporine. Sirolimus European Renal Transplant Study Group. *Transplantation.* 1999; 67: 1036-1042.

12. European Mycophenolate Mofetil Cooperative Study Group. Placebo-controlled study of mycophenolate mofetil combined with cyclosporine and corticosteroids for prevention of acute rejection. *Lancet.* 1995; 345: 1321-1325.

13. Sellares J, De Freitas D, Mengel M, et al. Understanding the causes of kidney transplant failure: the dominant role of antibody-mediated rejection and non-adherence. *Am J Transplant.* 2012; 12: 388-399.

14. Valenzuela NM, Elaine FR. Antibodies in transplantation: The effects of HLA and non-HLA antibody binding and mechanisms of injury. *Methods Mol Biol*. 2013; 1034: 41-70.

15. Schinstock C, Stegall M, Cosio F. New insights regarding chronic antibody-mediated rejection and its progression to transplant glomerulopathy. *Curr Opin Nephrol Hypertens*. 2014; 23: 611–618.

16. Sis B, Campbell PM, Mueller T, et al. Transplant glomerulopathy, late antibody-mediated rejection and the ABCD tetrad in kidney allograft biopsies for cause. *Am J Transplant.* 2007; 7: 1743-1752.

17. Remport A, Ivanyi B, Mathe Z, et al. Better understanding of transplant glomerulopathy secondary to chronic antibody-mediated rejection. *Nephrol Dial Transplant.* 2014; 30: 1825–1833.

18. Husain S, Sis B. Advances in the understanding of transplant glomerulopathy. *Am J Kidney Dis.* 2013; 62: 352-363.

19. Filippone EJ, McCue PA, Farber JL. Transplant glomerulopathy. *Mod Pathol.* 2018; 31: 235-252.

20. Cosio FG, Gloor JM, Sethi S, Stegall MD. Transplant glomerulopathy. *Am J Transplant.* 2008; 8: 492-496.

21. Habib R, Broyer M. Clinical significance of allograft glomerulopathy. *Kidney Int Suppl*. 1993; 43: S95-S98.

22. Maryniak RK, First MR, Weiss MA. Transplant glomerulopathy: Evolution of morphologically distinct changes. *Kidney Int*. 1985; 27: 799-806.

23. Sijpkens YW, Joosten SA, Wong MC, et al. Immunologic risk factors and glomerular C4d deposits in chronic transplant glomerulopathy. *Kidney Int*. 2004; 65: 2409-2418.

24. Suri DL, Tomlanovich SJ, Olson JL, et al. Transplant glomerulopathy as a cause of late graft loss. *Am J Kidney Dis*. 2000; 35: 674-680.

25. Vongwiwatana A, Gourishankar S, Campbell PM, et al. Peritubular capillary changes and C4d deposits are associated with transplant glomerulopathy but not IgA nephropathy. *Am J Transplant*. 2004; 4: 124-129.

26. Gloor JM, Sethi S, Stegall MD, et al. Transplant glomerulopathy: Subclinical incidence and association with alloantibody. *Am J Transplant*. 2007; 7: 2124-2132.

27. Gloor JM, Cosio FG, Rea DJ, et al. Histologic findings one year after positive crossmatch or ABO blood group incompatible living donor kidney transplantation. *Am J Transplant.* 2006; 6: 1841-1847.

28. Kieran N, Wang X, Perkins J, et al. Combination of peritubular C4d and transplant glomerulopathy predicts late renal allograft failure. *J Am Soc Nephrol.* 2009; 20: 2260–2268.

29. Einecke G, Sis B, Reeve J, et al. Antibody-mediated microcirculation injury is the major cause of late kidney transplant failure. *Am J Transplant.* 2009; 9: 2520-2531.

30. Redfield R, Ellis T, Zhong W, et al. Current outcomes of chronic active antibody-mediated rejection - a large single center retrospective review using the updated Banff 2013 criteria. *Hum Immunol.* 2016; 77: 346–352.

31. Patri P, Seshan S, Matignon M, et al. Development and validation of a prognostic index for allograft outcome in kidney recipients with transplant glomerulopathy. *Kidney Int.* 2015; 89: 450–458.

32. Kamal L, Broin P, Bao Y, et al. Clinical, histological, and molecular markers associated with allograft loss in transplant glomerulopathy patients. *Transplantation.* 2015; 99: 1912–1918.

33. Eng H, Bennett G, Chang S, et al. Donor human leukocyte antigen specific antibodies predict development and define prognosis in transplant glomerulopathy. *Hum Immunol.* 2011; 72: 386–391.

34. Hayde N, Bao Y, Pullman J, et al. The clinical and genomic significance of donor-specific antibody-positive/C4d-negative and donor-specific antibody-negative/C4d-negative transplant glomerulopathy. *Clin J Am Soc Nephrol.* 2013; 8: 2141–2148.

35. Lesage J, Noël R, Lapointe I, et al. Donor-specific antibodies, C4d and their relationship with the prognosis of transplant glomerulopathy. *Transplantation.* 2014; 99: 69–76.

36. John R, Konvalinka A, Tobar A, et al. Determinants of long-term graft outcome in transplant glomerulopathy. *Transplantation.* 2010; 90: 757–764.

37. Baid-Agrawal S, Farris AB, Pascual M, et al. Overlapping pathways to transplant glomerulopathy: Chronic humoral rejection, hepatitis C infection, and thrombotic microangiopathy. *Kidney Int*. 2011; 80: 879-885.

38. Loupy A, Jordan SC. Transplantation: donor-specific HLA antibodies and renal allograft failure. *Nat Rev Nephrol.* 2013; 9: 130–131.

39. Hidalgo LG, Campbell PM, Sis B, et al. De novo donor-specific antibody at the time of kidney transplant biopsy associates with microvascular pathology and late graft failure. *Am J Transplant.* 2009; 11: 2532-2541.

40. Loupy A, Hill GS, Suberbielle C, et al. Significance of C4d Banff scores in early protocol biopsies of kidney transplant recipients with preformed donor-specific antibodies. *Am. J. Transplant.* 2011; 11: 56–65.

41. Hickey MJ, Valenzuela NM, Reed EF. Alloantibody generation and effector function following sensitization to human leukocyte antigen. *Front Immunol.* 2016; 7: 30.

42. Wehner J, Morrell CN, Reynolds T, Rodriguez ER, Baldwin WM III. Antibody and complement in transplant vasculopathy. *Circ Res.* 2007; 100: 191–203.

43. Mauiyyedi S, Della Pelle P, Saidman S, et al. Chronic humoral rejection: Identification of antibody-mediated chronic renal allograft rejection by C4d deposits in peritubular capillaries. *J Am Soc Nephrol.* 2001; 12: 574-582.

44. Venner JM, Hidalgo LG, Famulski KS, Chang J, Halloran PF. The molecular landscape of antibody-mediated kidney transplant rejection: Evidence for NK involvement through CD16a Fc receptors. *Am J Transplant.* 2015; 15: 1336-1348.

45. Parkes MD, Halloran PF, Hidalgo LG. Evidence for CD16a-mediated NK cell stimulation in antibody-mediated kidney transplant rejection. *Transplantation*. 2017; 101: e102-e111.

46. Hidalgo LG, Sis B, Sellares J, et al. NK cell transcripts and NK cells in kidney biopsies from patients with donor-specific antibodies: evidence for NK cell involvement in antibody-mediated rejection. *Am J Transplant.* 2010; 10: 1812–1822.

47. Hidalgo LG, Sellares J, Sis B, et al. Interpreting NK cell transcripts versus T cell transcripts in renal transplant biopsies. *Am J Transplant* 2012; 12: 1180–1191.

48. Valenzuela NM, Reed EF. Antibodies to HLA molecules mimic agonistic stimulation to trigger vascular cell changes and induce allograft injury. *Curr Transplant Rep*. 2015; 2: 222–232.

49. Jin YP, Fishbein MC, Said JW, et al. Anti-HLA class I antibody-mediated activation of the PI3K/Akt signaling pathway and induction of Bcl-2 and Bcl-xL expression in endothelial cells. *Hum Immunol.* 2004; 65: 291–302.

50. Le Bas-Bernardet S, Coupel S, Chauveau A, Soulillou JP, Charreau B. Vascular endothelial cells evade apoptosis triggered by human leukocyte antigen-DR ligation mediated by allospecific antibodies. *Transplantation.* 2004; 78: 1729–1739.

51. Narayanan K, Jaramillo A, Phelan DL, Mohanakumar T. Pre-exposure to sub-saturating concentrations of HLA class I antibodies confers resistance to endothelial cells against antibody complement-mediated lysis by regulating Bad through the phosphatidylinositol 3-kinase/Akt pathway. *Eur J Immunol.* 2004; 34: 2303–2312.

52. Zhang X, Rozengurt E, Reed EF. HLA class I molecules partner with integrin beta4 to stimulate endothelial cell proliferation and migration. *Sci Signal.* 2010; 3: ra85.

53. Yamakuchi M, Kirkiles-Smith NC, Ferlito M, et al. Antibody to human leukocyte antigen triggers endothelial exocytosis. *Proc Natl Acad Sci U S A.* 2007; 104: 1301–1306.

54. Valenzuela NM, Hong L, Shen XD, et al. Blockade of p-selectin is sufficient to reduce MHC I antibody-elicited monocyte recruitment in vitro and in vivo. *Am J Transplant.* 2013; 13: 299–311.

55. Valenzuela NM, Mulder A, Reed EF. HLA class I antibodies trigger increased adherence of monocytes to endothelial cells by eliciting an increase in endothelial P-selectin and, depending on subclass, by engaging FcgammaRs. *J Immunol* 2013; 190: 6635–6650.

56. Wavamunno M, O'Connell P, Vitalone M, et al. Transplant glomerulopathy: Ultrastructural abnormalities occur early in longitudinal analysis of protocol biopsies. *Am J Transplant.* 2007; 7: 2757–2768.

57. Haas M, Mirocha J. Early ultrastructural changes in renal allografts: Correlation with antibody-mediated rejection and transplant glomerulopathy. *Am J Transplant.* 2011; 11: 2123–2131.

58. Böhmig GA, Exner M, Habicht A, et al. Capillary C4d deposition in kidney allografts: a specific marker of alloantibody-dependent graft injury. *J Am Soc Nephrol.* 2002; 13: 1091–1099.

59. Nickeleit V, Mihatsch MJ. Kidney transplants, antibodies and rejection: is C4d a magic marker? *Nephrol Dial Transplant.* 2003; 18: 2232–2239.

60. Satoskar AA, Pelletier R, Adams P, et al. De novo thrombotic microangiopathy in renal allograft biopsies – role of antibody-mediated rejection. *Am J Transplant.* 2010; 10:1804-1811.

61. K Solez, Axelsen RA, Benediktsson H, et al. International standardization of criteria for the histologic diagnosis of renal allograft rejection: The banff working classification of kidney transplant pathology. *Kidney Int.* 1993; 44: 411-421.

62. Racusen LC, Solez K, Colvin RB, et al. The banff 97 working classification of renal allograft pathology. *Kidney Int*. 1999; 55: 713-723.

63. Solez K, Colvin RB, Racusen LC, et al. Banff '05 meeting report: Differential diagnosis of chronic allograft injury and elimination of chronic allograft nephropathy. *Am J Transplant*. 2007; 7: 518-526.

64. Solez K, Colvin RB, Racusen LC, et al. Banff 07 classification of renal allograft pathology: Updates and future directions. *Am J Transplant*. 2008; 8: 753-760.

65. Haas M, Sis B, Racusen LC, et al. Banff 2013 meeting report: Inclusion of C4d-negative antibody-mediated rejection and antibody-associated arterial lesions. *Am J Transplant*. 2014; 14: 272-283.

66. Loupy A, Haas M, Solez K, et al. The banff 2015 kidney meeting report: Current challenges in rejection classification and prospects for adopting molecular pathology. *Am J Transplant*. 2017; 17: 28-41.

67. Haas M, Loupy A, Lefaucheur C, et al. The banff 2017 kidney meeting report: Revised diagnostic criteria for chronic active T cell-mediated rejection, antibody-mediated rejection, and prospects for integrative endpoints for next-generation clinical trials. *Am J Transplant*. 2018; 18: 293-307.

68. Hill GS, Nochy D, Bruneval P, et al. Donor-specific antibodies accelerate arteriosclerosis after kidney transplantation. *J Am Soc Nephrol.* 2011; 22: 975-983.

69. Liapis G, Singh HK, Derebail VK, Gasim AM, Kozlowski T, Nickeleit V. Diagnostic significance of peritubular capillary basement membrane multilaminations in kidney allografts: old concepts revisited. *Transplantation.* 2012; 94: 620-629.

70. Iványi B, Fahmy H, Brown H, Szenohradszky P, Halloran PF, Solez K. Peritubular capillaries in chronic renal allograft rejection: a quantitative ultrastructural study. *Hum Pathol.* 2000; 31: 1129-1138.

71. Ivanyi B, Kemeny E, Szederkenyi E, Marofka F, Szenohradszky, P. The value of electron microscopy in the diagnosis of chronic renal allograft rejection. *Mod Pathol*. 2001; 14: 1200-1208.

72. Iványi B. Transplant capillaropathy and transplant glomerulopathy: ultrastructural markers of chronic renal allograft rejection. *Nephrol Dial Transplant.* 2003; 18: 655-660.

73. Roufosse CA, Shore I, Moss J, et al. Peritubular capillary basement membrane multilayering on electron microscopy: a useful marker of early chronic antibody-mediated damage. *Transplantation.* 2012; 94: 269-274.

74. de Kort H, Willicombe M, Brookes P, et al. Peritubular capillary basement membrane multilayering in renal allograft biopsies of patients with de novo donor-specific antibodies. *Transplantation.* 2016; 100: 889-897.

75. Terasaki PI, McClelland JD. Microdroplet assay of human serum cytotoxins. *Nature.* 1964; 204: 998-1000.

76. Patel R, Terasaki PI. Significance of the positive crossmatch test in kidney transplantation. *N Engl J Med.* 1969; 280: 735–739.

77. Sis B, Einecke G, Chang J, et al. Cluster analysis of lesions in nonselected kideney transplant biopsies: microcirculation changes, tubulointerstitial inflammation and scarring. *Am J Transplant.* 2010; 10: 421-430.

78. Hall BM, Bishop GA, Duggin GG, Horvath JS, Philips J, Tiller DJ. Increased expression of HLA-DR antigens on renal tubular cells in renal transplants: relevance to the rejection response. *Lancet.* 1984; 2: 247-251.

79. Wen J, Zhang M, Chen J, Zeng C, Cheng D, Liu ZH. HLA-DR overexpression in tubules of renal allografts during early and late renal allograft injuries. *Exp Clin Transplant.* 11: 499-506.

80. Jensen E, Gundersen H, Osterby R. Determination of membrane thickness distribution from orthogonal intercepts. *J Microsc.* 1979; 115: 19–33.

81. Drumond M, Deen W. Structural determinants of glomerular hydraulic permeability. *Am J Physiol*. 1994; 266: F1–F2.

82. Drumond MC, Kristal B, Myers BD, Deen WM. Structural basis for reduced glomerular filtration capacity in nephrotic humans. *J Clin Invest*. 1994; 94: 1187-1195.

83. Youden WJ. Index for rating diagnostic tests. *Cancer. 1950;* 3: 32-35.

84. Levey AS, Eckardt KU, Tsukamoto Y, et al. Definition and classification of chronic kidney disease: a position statement from Kidney Disease: Improving Global Outcomes (KDIGO). *Kidney Int* 2005; 67: 2089-2100.

85. Kidney Disease: Improving Global Outcomes (KDIGO) CKD Work Group. KDIGO 2012 Clinical Practice Guideline for the Evaluation and Management of Chronic Kidney Disease. *Kidney Int.* Suppl. 2013; 3: 1–150.

86. Steffes M, Barbosa J, Basgen J, et al. Quantitative glomerular morphology of the normal human kidney. *Lab Invest.* 1983; 49: 82–86.

87. Haraldsson B, Nyström J, Deen W. Properties of the glomerular barrier and mechanisms of proteinuria. *Physiol Rev.* 2008; 88: 451–487.

88. Mengel M, Reeve J, Bunnag S, et al. Scoring total inflammation is superior to the current Banff inflammation score in predicting outcome and the degree of molecular disturbance in renal allografts. *Am J Transplant.* 2009; 9: 1859-1867.

89. Go H, Shin S, Kim Y, Han D, Cho Y. Refinement of the criteria for ultrastructural peritubular capillary basement membrane multilayering in the diagnosis of chronic active/acute antibody-mediated rejection. *Transplant Int.* 2017; 30: 398-409.

90. Galichon P, Xu-Dubois YC, Finianos S, Hertig A, Rondeau E. Clinical and histological predictors of long-term kidney graft survival. *Nephrol Dial Transplant* 2013; 28: 1362–1370.